Elucidation of the biochemical pathways involved in two distinct cut-surface discolouration phenotypes of lettuce

Elucidation of the biochemical pathways involved in two distinct cut-surface discolouration phenotypes of lettuce.

Paul J. Hunter[1], Martin Chadwick[2], Abigail Graceson[1], Angela Hambidge[3], Paul Hand[1], Jennifer Heath[1], Stella Lignou[2], Maria Jose Oruna-Concha[2], David Pink[1], Bindukala Rada[2], Carol Wagstaff[2], Guy Barker[3], James M. Monaghan[1*]

[1] Fresh Produce Research Centre, Harper Adams University, Newport, Shropshire TF10 8NB, UK

*corresponding author

jmmonaghan@harper-adams.ac.uk

[2]Department of Food and Nutritional Sciences, University of Reading, Harry Nursten Building, Pepper Lane, Whiteknights, Reading, RG6 6DZ, UK

[3] School of Life Sciences, University of Warwick, Gibbet Hill Road, Coventry, CV4 7AL, UK

Running Title: Biochemistry of lettuce pinking and browning

Abstract

To understand better the biochemistry and underlying genetic control of post-harvest discolouration in lettuce, an F_7 recombinant inbred population (Saladin x Iceberg) was grown in field trials and phenotyped. We identified two distinct discolouration phenotypes, pinking and browning, which were negatively correlated at the phenotypic

level and located six QTL associated with pinking and five QTL associated with browning plus two QTL associated with total discolouration which could not be attributed to either type, on an improved genetic map. Candidate genes underlying QTL were investigated. Plants showing extremes of discolouration were also grown under controlled environment conditions. Lines showing extreme phenotypes from both environments were used for transcriptome profiling and differentially expressed transcripts associated with pinking and browning were identified. Involvement of the phenylpropanoid, flavonoid and terpenoid biosynthesis pathways were indicated in the development of discolouration, with the point of divergence for development of the different discolouration phenotypes localised to the phenylpropanoid pathway. Other peripheral biochemistry including amino acid metabolism was also implicated with environmental factors including temperature, water availability and physical stress indicated as potential contributory factors. Differential transcriptional control may be involved in regulating discolouration, potentially through stereochemical selection.

KEYWORDS: Lettuce discolouration, pinking, browning, differentially expressed transcripts, QTL.

1 Introduction

Many leafy vegetables, including lettuce (*Lactuca sativa*), are susceptible to post-harvest discolouration. Minimal processing adds value to fresh produce (Soininen, 2009), but also increases perishability, reducing shelf life and increasing waste. “Pinking” or “browning” discolouration at the cut surface of processed lettuce due to the accumulation of pigmented compounds is believed to occur via action of polyphenol oxidases (PPO) on phenolic compounds from the phenylpropanoid pathway. This leads

to the formation of quinones which then polymerize, or react with amino acids and proteins to form pigments (Zawistowski *et al*., 1991; Martinez and Whitaker, 1995; Solomon *et al.,* 1996; Gawlik-Diziki *et al.,* 2008; Toivonen and Brummell 2008; García et al., 2018; Saltveit 2018; García et al., 2019). In healthy plant tissue PPO and polyphenolic compounds are separated by sub-cellular compartmentalization; PPO in the chloroplast and the majority of polyphenol products in the vacuole (Toivonen and Brummell, 2008). Mechanical damage during processing compromises this compartmentalization at the wound surface, allowing mixing of PPO and phenolic substrates (Kays, 1999; Hilton *et al.*, 2009; Degl'Innocenti *et al.,* 2005; Querioz *et al.*, 2008; Toivonen and Brummell, 2008).

Genetic variation (Atkinson *et al.,* 2013a) and the environment the plant encounters during growth (Lee and Kader, 2000) have both been shown to be major factors in determining postharvest quality and shelf-life of ready-to-eat lettuce. Environmental factors associated with discolouration include low temperature, nutrient (particularly nitrogen) availability, maturity at harvest, rainfall, temperature, light exposure (particularly UV), and potentially microbial colonization (Hunter *et al.,* 2017). Whilst improved processing techniques (including modified atmosphere packaging) can help reduce post-processing discolouration, an alternative strategy is to manipulate plant biochemistry either at a chemical or genetic level. In order for this to be effective, an in-depth understanding of the biochemical processes and the underlying genetic control of plant pathways involved is required.

In this study, we have used a set of F_7 recombinant inbred lettuce lines (RILs) with previously demonstrated variation in the development of pinking and browning discolouration. These RILs were grown in field trials and chopped, bagged and stored in a cooled environment typical of commercial practice. Discolouration was assessed

over a 3-day post-harvest storage period. Lines selected as showing consistently high and low levels of discolouration were also grown under controlled environment (CE) conditions and transcriptomic analyses of both field-grown and CE material were performed. In addition, quantification of discolouration phenotypes was used to locate QTL on a revised Saladin x Iceberg genetic map and putative candidate genes underlying QTL were identified.

2 Materials and Methods

2.1 Plant production – Field trials

The field studies utilised the 94 most informative lines of a *Lactuca sativa* Saladin x Iceberg RIL population (Atkinson *et al* 2013a) and parents. Field trials were conducted at Harper Adams University, Shropshire in central UK (Grid Ref SJ 711200) over three consecutive years (2015 - 2017). Multiple sowings were grown in each year (Table 1).

Table 1. Growth periods and average environmental conditions for each trial.

Year	Trial	Transplant Date	Harvest Date	Mean Daily Average Air Temperature (°C)
2015	1	16 June	25 August	15.6
	2	23 June	25 August	15.8
	3	30 June	26 August	15.8
2016	4	14 April	21 June	11.8
	5	10 May	5 July	14.1
	(6)	Trial abandoned		
	7	3 August	27 September	16.0
2017	8	6 June	31 July	16.2
	9	20 June	14 August	16.0

Plant production followed commercial practice. Seed were sown 1.5cm deep in pre-formed 3x3x4cm commercial peat plugs with a 0.5cm diameter hole (provided by G's Fresh, Cambridgeshire, UK). Seeds were covered with vermiculite, watered and maintained at 15°C in the dark until emergence. Emerged seedlings were transferred to a mesh sided polytunnel under ambient temperature and light until they reached the 3-4 true leaf growth stage (approximately two weeks). Seedlings were then transplanted into prepared field plots.

Field plots were sub-soiled to a depth of 40cm, ploughed to a depth of 20cm and power-harrowed to a depth of 10cm using a power-harrow fitted with packer-roller. Soil samples were taken for moisture and nutrient analyses and the results used to calculate nutrient input (Defra, 2010). A top-dressing of an additional 50kg/Ha N was applied 2 weeks post-transplanting. In addition, pre-emergence herbicides Stomp-Aqua (BASF) and Wing-P (BASF) were applied at1L/Ha and 1.25L/Ha respectively in the 2015 and 2016 trials.

Seedlings were transplanted into randomized trials in blocks of 12 plants per line in a 3x4 grid in 2015 and 2016 and blocks of 6 plants per line in a 2x3 grid in

2017. Spacing was 40cm between planting stations in 2015 and 60cm between stations in 2016 and 2017. Trials were irrigated with overhead spray in 2015 and drip tape in 2016 and 2017 to maintain commercially recommended soil moisture levels (ADAS, 2007).

Metaldehyde slug pellets were applied at transplanting and re-applied as necessary. Fungicide protection was achieved with 2kg/Ha Karamate (Indofil Industries B.V., Amsterdam, Netherlands.) with 0.8kg/Ha Switch (Syngenta UK Ltd, Fulbourn, UK) at 7 days post-transplanting, 2kh/Ha Invader (BASF (UK), Littlehampton UK) with 1.5kg/Ha Signum (BASF) at 17 days post-transplanting, 1.9kg/Ha Fubol Gold (Syngenta) with 0.5L/Ha Movento (Bayer AG, Monheim am Rhein, Germany) at 27 days post-transplanting (with the additional inclusion of 0.075L/Ha Hallmark (Syngenta) if disease pressure was considered high), and 0.6L/Ha Revus (Syngenta) with 250mL/Ha Decis (Bayer) at 37 days post-transplanting.

2.2 Plant production – CE

Lines exhibiting consistently high or low pinking or browning responses were identified based on the 2015 and 2016 field trials and previous work (Atkinson *et al.,* 2013a) and plants of these lines were also grown in controlled environment (CE) over winter in 2016 (Table 2). Seeds were sown into Levington F2S compost (Scotts Professional, Ipswich, UK) in 5x8 cell modular trays (Plant Pak P40, Desch Plantpak Ltd, Maldon, UK) and kept in the dark at 15^{o}C until emergence. Three replicate seedlings of each were then potted on into 1L pots of M2 compost (Levington) amended with 2g/L Osmocote (ICL group, Tel Aviv, Israel) slow release NPK fertiliser. Seedlings were randomly arranged in a CE cabinet (Weiss Technik UK Ltd,

133 Loughborough, UK) and maintained under a 16h day / 8 hr night light cycle, 18ºC /15ºC

134 (day / night) temperature, 90% RH and ambient CO_2.

135
136

137

Table 2. Lines exhibiting consistently high or consistently low pinking or browning responses used for RNA extraction.

Plants Grown in CE (2016)

		Average Pinking Index Value		
Line	**Phenotype**	**2015**	**2016**	**2017**
10045	**HP**	166.7	93.9	106.9
10055	**HP**	236.1	155.5	152.8
10095	**HP**	175.5	63.3	175.0
10023	**LP**	31.5	19.3	8.3
10043	**LP**	26.9	3.8	17.5
10073[a]	**LP**	10.2	3.8	13.4

		Average Browning Index Values		
Line	**Phenotype**	**2015**	**2016**	**2017**
10022[b]	**HB**	189.8	95.7	128.1
10053[c]	**HB**	106.5	39.6	168.8
10069	**HB**	149.1	27.3	124.3
10043	**LB**	57.4	44.0	64.1
10045	**LB**	79.6	25.2	113.4
10051	**LB**	59.3	13.0	50.2

Additional Field Grown Lines (2016)

		Average Pinking Index Value		
Line	**Phenotype**	**2015**	**2016**	**2017**
10088[d]	**LP**	67.1	15.8	83.5

		Average Browning Index Values		
Line	**Phenotype**	**2015**	**2016**	**2017**
10029[e]	**HB**	117.8	91.7	128.3
10030[f]	**HB**	141.9	43.1	110.4

138 HP: lines showing consistently high levels of pinking, LP: lines showing consistently low levels of
139 pinking, HB: lines showing consistently high levels of browning, LB: lines showing consistently low
140 levels of browning. [a,b,c]: lines not available for RNASeq analysis from field material due to poor quality
141 RNA, [d,e,f]: the replacement field lines used for transcriptome analysis

142

2.3 Harvest and processing

In the field trials, the central two heads in each block were harvested at maturity, the remaining heads acting as guard plants. The two heads were treated as separate samples. Heads were cut in the morning and transferred to 5ºC to remove field heat. The outer (wrapper) leaves were removed before heads were quartered longitudinally, the core removed and leaf material cut into approximately 3x3cm pieces. Cut material was mixed and approximately 100g of material transferred to each of three commercial unperforated pillow pack bags (Amcor 35PA240; Amco Flexibles, Bristol, UK). Bags were heat sealed and placed into cold storage at 5ºC in the dark. Replicate bags were removed from cold storage after approximately 2 hours (0 days post-harvest), 1 day and 3 days and discolouration recorded. Recorded samples were then transferred to -80ºC for long term storage. In the CE trials, plants were harvested at 8 weeks post-transplanting, processed, stored and recorded in the same manner as the field grown material.

2.4 Scoring of discolouration

Pillow packs were overlaid with a 3x4 grid composed of 12 6x6 cm squares. Pinking and browning symptoms were scored separately in each square on a 5-point system based on photographic standards reported in Hilton *et al*. (2009), as used by Atkinson *et al.* (2013a); 0 – no appearance of discolouration, 1 – slight discolouration but unable to differentiate between pinking or browning (a score of 1 for both symptoms), 2 – low level discolouration (pinking or browning), 3 – intermediate discolouration, 4 severe discolouration. An average score for each symptom for each bag (symptom intensity) was recorded. The percentage of grid squares showing symptoms was also recorded

167 (symptom distribution) and a symptom index calculated as a product of the intensity
168 and distribution.
169
170 2.5 Mapping and QTL analysis
171 In order to improve the marker density of the previously published Saladin x Iceberg
172 linkage map (Atkinson *et al.,* 2013b), additional KASP markers were derived from
173 single nucleotide polymorphisms (SNPs) between the genomic sequences of the
174 parents. For SNP identification total RNA extracts were made from each parental line
175 and mRNA selected using oligo(dT) Dynal magnetic beads (Invitrogen, MA, USA)).
176 The integrity of RNA was confirmed on a Bioanalyser (Agilent Technologies LDA UK
177 Ltd, Stockport, UK). TruSeq (Illumina Inc., San Diego, CA, USA) libraries prepared
178 from this material were sequenced on a HiSEQ (Illumina) platform to produce 70nt
179 single end reads.
180 A lettuce reference sequence database was constructed comprising candidate
181 genes for the phenylpropanoid pathway, leaf senescence, nitrate use efficiency,
182 flowering time, and ESTs from the CLS_S3_Sat.assembly (L. sativa|CAP3:100/95)
183 database (http://cgpdb.ucdavis.edu/cgpdb2/est_info_assembly.php). Reads were base-
184 called and scored for read quality and aligned to the reference EST sequences using
185 Bowtie v0.11.3 (Langmead *et al*., 2009), and consensus sequences generated for each
186 accession using SAMtools (Li *et al*., 2009). SNP loci were then identified between
187 consensus sequences using a custom Perl pipeline. Loci with very low coverage or
188 sequencing quality (Phred score < 33) in either accession were discounted. Unique
189 SNPs amenable to unambiguous PCR were identified by aligning 150nt regions of the
190 consensus sequence around each SNP to the reference database using BLAST (Altschul
191 *et al.,* 1990) at >98 % identity. This resulted in 1395 SNPs from which 682 unique

KASP markers were developed. 78 potential markers were eliminated in quality checks resulting in 604 additional KASP markers. Combined with the data from the previous version of the map, the extended lettuce mapping dataset contained 1028 loci scored over 108 individuals from the Saladin x Iceberg F_7 population. A linkage map was constructed using the Kosambi mapping function (LOD threshold 0.01, recombination frequency threshold 0.49, jump threshold 5.0, ripple value 1) in Joinmap 4.0 (Van Ooijen, 2018). Loci were grouped using Independence LOD and mapping groups were selected at LOD 5-6. Loci with high recombination frequency and LOD score or with SCL values > 5.0 were excluded.

Each 100bp region containing a SNP was aligned to a pseudo-chromosome genomic locus from a draft *L. sativa* genome assembly 'Lsat_1_v4', accessed from the U.C. Davis lettuce genome resource site (http://lgr.genomecenter.ucdavis.edu). The assembly comprises 1.5 Gb of sequence as 9 pseudo-chromosomes. Unmapped SNPs were included as an additional group. The final map contained 27 groups aligned with lettuce pseudo-chromosomes using KASP markers. 2 groups could not be aligned with lettuce pseudo-chromosomes due to lack of corresponding markers.

For QTL analyses, discolouration severity and index values were logarithmically transformed according to the formula v=ln(x+2) and discolouration distribution and qRT-PCR expression values (%) were ArcSine transformed prior to analysis. QTL analysis was conducted using MapQTL v6 (Van Ooijen, 2009). Initial QTL were positioned using a combination of Kruskal-Wallace and Interval Mapping using data across all available trials. Initial QTL locations were used as cofactors for subsequent multiple QTL model (MQM) analyses. MQM analyses were conducted iteratively with each round of QTL locations being used as cofactors in the subsequent round until no further movement in QTL positions occurred. In all cases the head

morphotype was included as a co-variant to exclude morphology effects. Significant QTL were identified based on LOD scores above the genome wide LOD threshold calculated according to the Permutation Test protocol of the software. Genes underlying QTL with at least a one base overlap of the QTL region were identified using Bedtools (Quinlan and Hall, 2010), with gene locations determined from the U.C. Davis Lettuce Genome Resource (http://lgr.genomecenter.ucdavis.edu/). Six-frame translations of the genes were generated using the EMBOSS tranSeq tool (Maderira *et al.,* 2019). Annotation was added by comparing these translations against the NCBI RefSeq Non-Redundant proteins database (Pruitt *et al.,* 2005), using DIAMOND (Buchfink *et al.,* 2015) in the 'more-sensitive' mode with an e-value cut-off of 0.001. Predicted function and family membership was determined by searching for functional regions in the translations using InterProScan (Jones *et al.,* 2014).

2.6 RNA extraction and transcription profiling

Frozen plant material from trials 5 and 7, and from CE plants, was freeze-dried and milled to a homogeneous powder. 50-60mg was extracted using the FastRNA Green protocol (MP Biomedical, Santa Ana, CA, USA), with a 40sec homogenization at setting 6.0 on the FastPrep homogenizer and the inclusion of a second chloroform extraction. Extracted RNA was re-suspended in 100µl of DEPC-treated water and further purified using the RNeasy Mini RNA clean up protocol (Qiagen UK Ltd, Manchester, UK) with elution in 60µl of sterile nuclease-free water (Invitrogen). RNA concentration was determined using a Qubit fluorometer (Invitrogen) with the RNA high sensitivity (HS) buffer system. Quantified RNA was stored at -80^{o}C for further use.

241 For transcription profiling, TruSeq RNA (Illumina) libraries were prepared
242 from RNA of field grown plants representing the identified consistently high and low
243 discolouring lines (Table 2) in trials 5 and 7. Additional libraries were prepared from
244 RNA of these lines grown under CE conditions (12 lines x 3 time points). Libraries
245 were sequenced as for the mapping (above) with the exception that 150bp single end
246 reads were generated to an approximate depth of 30 million reads per library.
247 Reads were quality checked using Fastqc (Andrews, 2010) and MultiQC (Ewels
248 *et al.,* 2016). Adapters and poor-quality sequence ("quality 20") were removed using
249 CutAdapt (Martin, 2011). PhiX control sequences were removed using BBduk
250 (Bushnell) with arguments "k=31" and "hdist=1". Reads were aligned to the lettuce
251 genome using STAR (Dobin *et al.,* 2013) with a "sjdbOverhang" parameter of 149. The
252 lettuce genome (ID 35223) was downloaded from CoGe (Lyons and Freeling, 2008)
253 and annotated with similarity, protein function and orthology using DIAMOND
254 (Buchfink *et al.,* 2015) and InterProScan (Jones *et al.,* 2014) as above and with
255 EggNOG-mapper (Huerta-Cepas *et al.,* 2017) using the eukaryote database "euNOG"
256 with 1:1 orthologs and "Experimental Only" Gene Ontology evidence. Uniquely
257 mapped reads were counted using FeatureCounts (Liao *et al.,* 2014) with argument "-s
258 2" and analysed in DESeq2 (Love *et al.,* 2014) with default settings, in R v 3.2.3 (R
259 core team, 2018). Trials 5, 7 and the CE samples were analysed separately. Differential
260 expression was tested between pooled data representing high and low pinking and
261 browning, and also between samples representing high and low expression of pinking
262 and browning. Functional enrichment of Gene Ontology, KEGG Orthology and Cluster
263 of Orthologous Groups terms from EggNOG-mapper gene annotations was determined
264 using the goseq package (Young *et al.,* 2010). For this enrichment analysis, a
265 significance cut-off of Benjamini-Hochberg adjusted P value less than 0.1 was used to

266 determine the differentially expressed genes. A maximum P value of 0.1 was also used
267 for significant enrichment of function terms. Following analysis, transcripts were
268 selected which showed 3-fold or greater expression level differences consistently across
269 the two field trials or the three CE replicates. Transcripts which did not generate a
270 predicted protein sequence or a sequence that could not be identified by homology were
271 excluded.
272
273 2.7 qRT-PCR
274 Primers were designed for target transcripts from sequences located on the lettuce
275 genome sequence assembly 'Lsat_1_v8', (http://lgr.genomecenter.ucdavis.edu). Gene
276 and cDNA sequences were aligned to identify intron regions. Primers for 100-200bp
277 amplicons were designed with one primer extending across an intron excision site
278 where possible, to ensure no unintentional amplification signal from contaminating
279 genomic DNA (Table S1). Primers were tested on RNA extracts from the parent plants
280 of the cross, the optimum annealing temperatures determined and the resulting
281 amplicons sequenced to confirm target identity.

Table S1. Primer sequences and associated melting temperatures (Tm) and reaction annealing temperatures (Tann) used for qRT-PCR studies.

Target	Forward primer sequence	Tm (oC)	Reverse primer sequence	Tm (oC)	Tann (oC)
Absicic acid hydrolase 4	atgccaattacgtacaaggtgatat*	59	aacttcccagcttaacaactccta	61	56
Chalcone synthase	gcgcatgtgtgacaagtctatg*	63	aagaaatggctcgaacccctgaag	64	58
Phenylaniline ammonia lyase	agttaaggcgagtagtgattgggtt*	63	tttagattactcgaggaagaca	57	52
Polyphenol oxidase[a]	cacaaatattctcgacttcaaacca		ctcggtagcgttatgcgtgtt		
Trans-cinnamate 4-monooxygenase	catcaacgttgctgcaatcgaaaca*	63	tgccagacctccatcccctcaaaac	68	58
Chalcone-flavonone isomerase	aggtatctgaaatgtgcgttggtg	63	agctcttcgactaactttcactt*	59	54
Flavonoid-3'-monooxygenase	cgctagcagaccaccgaactcc	68	cgatggaggaggacggcttgc*	68	63
NAD(P)H-quinone oxidoreductase	ttcttggcaggaacgagttatgata	61	ttcttttaagacgttgttttggtga*	58	53
Reference sequences					
Actin12[a]	acctcagcagaacgtgaaattgtaa	61	gagcattgagaagagttgtctgctt	63	56
Protein phosphatase 2A regulatory subunit A3	catgcaatggttacaagacaaggtat*	61	gtttgaggaggcgttcagagaag	64	56
TIP41	tttgtatggagatgaattggctgata	61	ccatcaactctaagccagaaacgt*	63	56

*primers designed across exon / intron boundaries, [a] gene sequence did not contain intron regions

For qRT-PCR, 250ng of RNA from each field sample from trials 5 and 7 was first denatured for 5 min at 65°C in the presence of 250ng oligo$(dT)_{12-18}$ reverse primer (Invitrogen). First strand cDNA synthesis for 50 min at 42°C, followed by incubation for 15 min at 72°C in the presence of 1mM (each) dNTPs, 12mM dithiothreitol, 100 units of Superscript II reverse transcriptase (Invitrogen) and 20 units of RNAse OUT RNAse inhibitor (Invitrogen) followed by cooling to 4°C. In addition, multiple cDNA samples from parental material were combined for use in preparing a standard curve for quantitation. Standards of 10^0 x – 10^{-4} x relative concentrations of this material were produced by 10-fold serial dilution. Triplicate samples of 1µl of each cDNA amplification and standard curve dilution and a blank of 5µl of sterile nuclease free water were combined with 5µl 2x SensiFast Sybr No-ROX reagent (Bioline Reagents Ltd. London UK), and 1µl each of 3µM target specific forward and reverse primer in a LightCycler 480 multiwell 384 well plate (F. Hoffman-La Roche (UK) Ltd, Welwyn Garden City, UK) sealed with a ThermalSeal RT sealing film (Excel Scientific Inc. Victorville CA, USA) qRT-PCR was performed in a LightCycler 480 (Roche) as follows; 3 min denaturation at 95°C followed by 45 amplification cycles of 5 sec at 95°C, 10 sec at the appropriate annealing temperature for the primer pairs (Table S1) and 10 sec extension at 72°C with a single fluorescence acquisition. Following amplification, the melting temperature of the amplicon was determined by denaturing for 5 sec at 95°C, re-associating the product for 1 min at 65°C then increasing temperature at 0.11°C / sec to 97°C with 5 fluorescence acquisitions per second. Amplification was quantified against the relative standard curve using the Absolute quantification / 2nd derivative maximum method and the *Tm*-calling protocol was used to determine amplicon melting temperatures for all wells.

Results which did not fit the melting temperature profile for the appropriate amplicon were discarded. Any signal detected in the averaged blank wells was subtracted from the signal in the sample wells before further data processing. Mean signal values were calculated for each triplicate sample. Expression of actin 12, actin 2, alpha tubulin 3, protein phosphatase 2A regulatory subunit A3 (PP2AA3) and TIP41 (41kDa TAP42 interacting protein) (Sgamma *et al.,* 2016) were compared for use as internal references. Actin 12, PP2AA3 and TIP41 showed the lowest variation in transcript levels across the RILs and were selected as controls. Values from replicate samples were compared for each of these referents and showed no significant variation between RILs, furthermore ANOVA between the 50% of samples representing the highest and lowest averaged discolouration indices (for both pinking and browning separately) also showed no significant differences in reference gene expression indicating suitability for use as a normalization standard. All subsequent data was normalized against a geometric mean of the arithmetic mean data from these transcripts.

3 **Results and Discussion**

3.1 Discolouration Phenotype

Mean discolouration intensity scores, percentage incidence and severity indices for both pinking and browning were calculated from data from all eight field trials. Average index values showed considerable transgressive segregation in the RILs compared to the parent lines (Figure 1). Data for intensity scores and percentage incidence followed a similar pattern (not shown). The fact that this transgressive segregation can be observed in data averaged from eight separate trials suggests that it is predominantly genetic in nature rather than an environmental response.

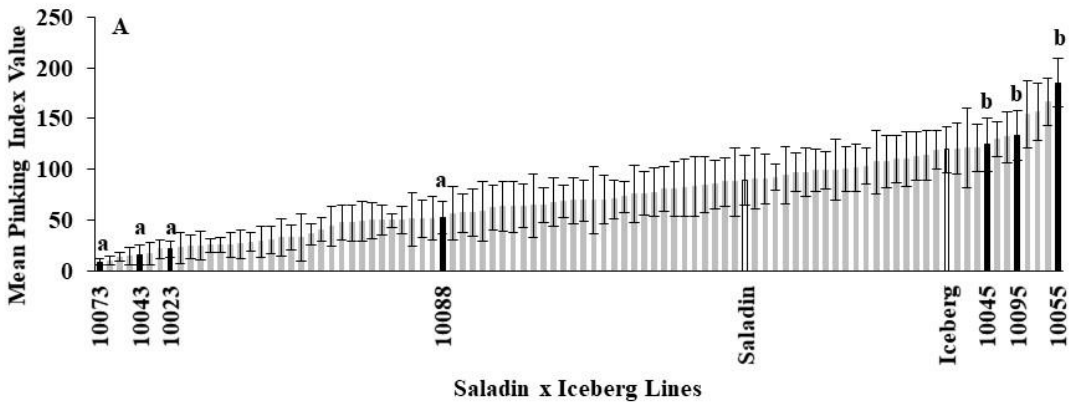

335

336

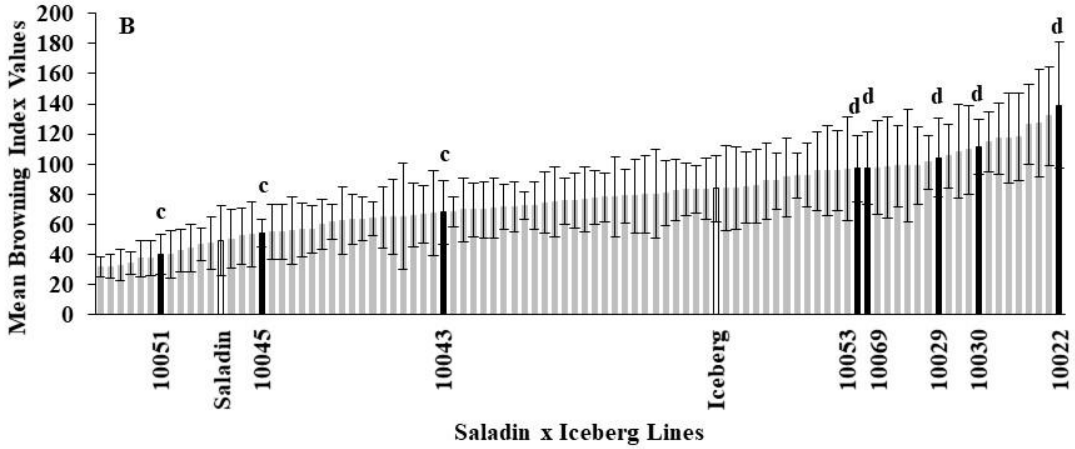

337

338 **Figure 1.** Distribution of mean pinking (1A) and browning (1B) index values across
339 the 94 lines of the Saladin x Iceberg RIL population. Parental lines are indicated by
340 white bars; the population shows considerable transgressive segregation for both
341 symptoms. Black bars indicate average index values across all trials for lines selected
342 after 2015 trials as consistently low pinking (a) and browning (c) and high pinking (b)
343 and browning (d) lines. Error bars show standard error of the mean values.

344

345

346

There was a significant dichotomy in mature head morphology noted in the RILs with 49% having a compact head type similar to Iceberg lettuce, whilst 51% had a looser head type similar to a Cos variety, however no statistically significant difference in the intensity or incidence of pinking or browning was detected between the two morphotypes. Examination of the relationship between pinking and browning discolouration revealed a significant negative correlation ($p<0.001$) between the two types of discolouration (Figure 2). Data from longer term studies conducted over 6 days in trials 1-3 (not shown), suggests that whilst pinking and browning became more intense and/or more widespread over time, the relative proportion of the different types of discolouration symptoms did not change significantly as would be expected if discolouration were progressing from one state to another, indicating that the two types of discolouration result from separate, but related, processes.

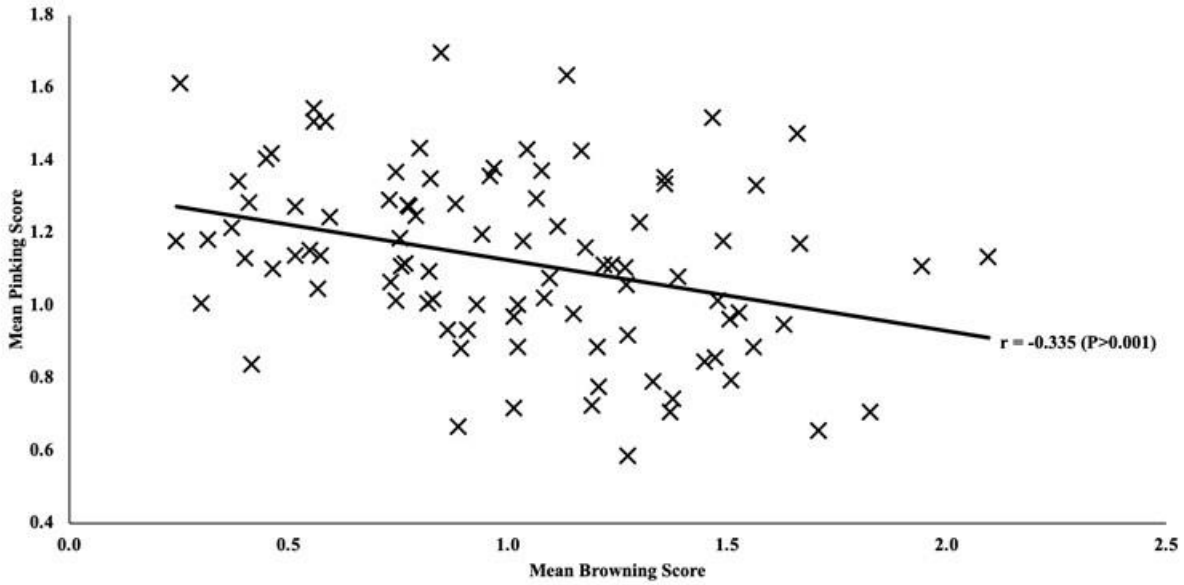

Figure 2.

Scatter plot indicating a negative correlation between pinking and browning discolouration intensity. The intensity scores are averaged for each of the 94 RIL accession across all trials. The trendline indicates a Pearson's correlation coefficient (r) of -0.335 corresponding to a significant negative correlation at $p<0.001$. Data for percentage incidence and severity index show similar significant trends (data not shown).

3.2 QTL mapping

QTL mapping of the discolouration phenotypes identified six QTL for pinking and five QTL for browning, (Figure 3) accounting for 58% and 73% of observed variation respectively. Two additional QTL for overall discolouration were also identified. The identification of separate QTL for pinking and browning supports the suggestion that the two types of discolouration are biochemically different. A QTL study of processed lettuce decay in modified atmosphere packaging conditions (Hayes *et al*., 2014) identified three QTL for decay with the most significant located on linkage group (LG) 4 and minor QTL on LG 1 and 9a. We identified no QTL on LG 4 of the Saladin x Iceberg map however, and those that did locate to LG 1 and LG 9 were not in the same positions, with the decay QTL identified by Hayes *et al.,* locating to the middle of LG 1 and the very top end of LG 9a. Hayes *et al.* (2014) used a map derived from a slightly different cross, Salinas 88 (derived by backcrossing lettuce mosaic virus resistance into Salinas which is synonymous with Saladin) x La Brilliante. Whilst QTL positions are therefore not directly comparable, the disparity between the QTL locations, especially the lack of a QTL on LG 4 corresponding to the major decay QTL reported by Hayes *et al.* (2014), suggest that it is unlikely that the QTL identified in the current study represent anaerobic decay.

389 Figure 3

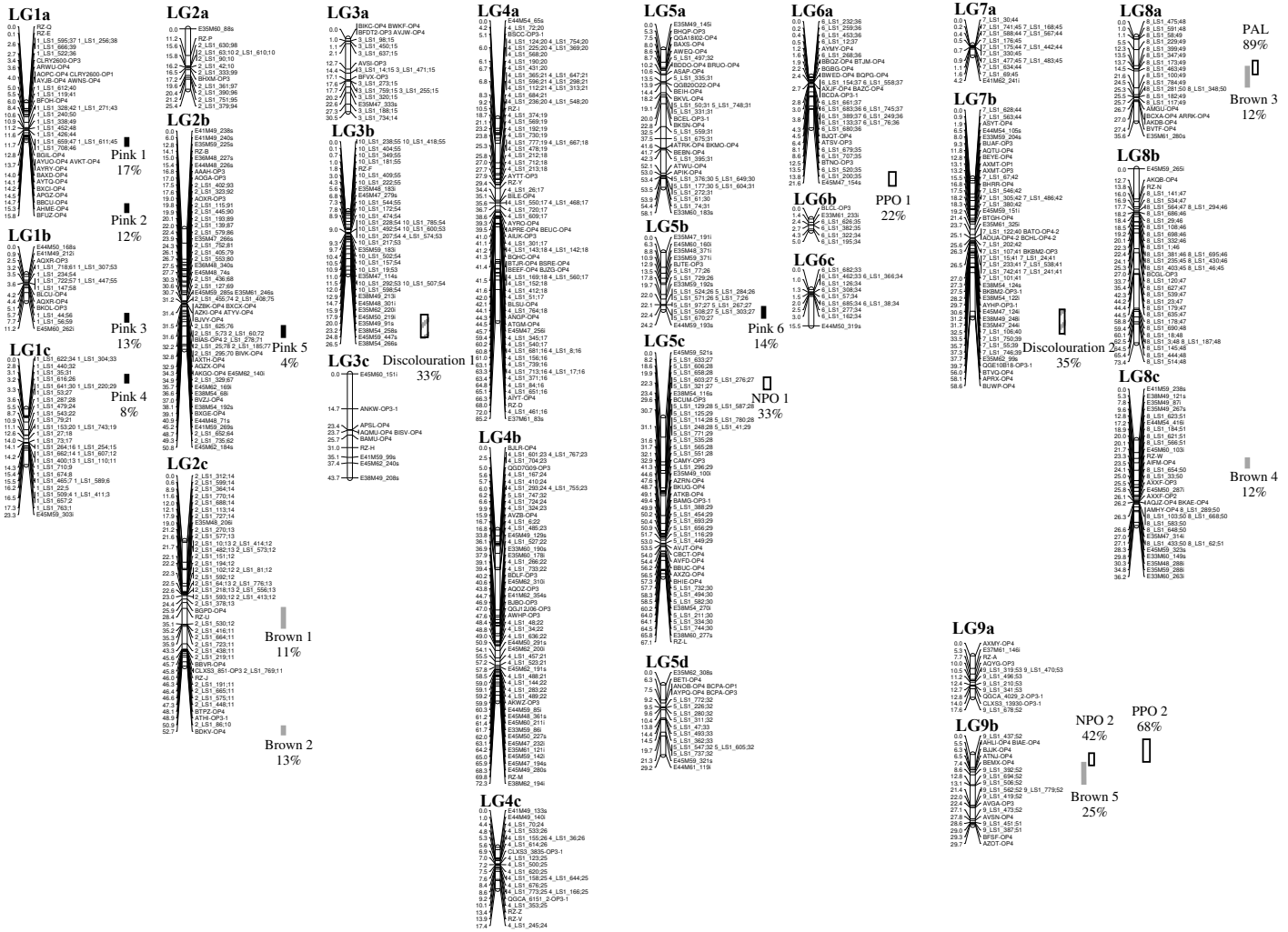

390

391 **Figure 3.** Revised linkage map of *L. sativa* Saladin x Iceberg. The map consists of 26
392 linkage groups organized into pseudochromosomes. Mapping produced one additional
393 linkage group of unassociated markers and a number of un-linked markers (not shown
394 as no QTL located to these groups) QTL are identified by vertical bars. Solid black bars
395 indicate QTL associated with pinking (Pink 1-6), grey bars indicate QTL associated
396 with browning (Brown 1-5), hatched bars indicate QTL associated with overall
397 discolouration (Discolouration 1-2) not attributable to either pinking or browning.
398 These QTL are produced from data from all eight field trials. White bars indicate the
399 positions of QTL mapped from data from trials 5 and 7 for the qRT-PCR targets which
400 showed potential co-location with discolouration QTL (PAL = phenylalanine ammonia
401 lyase, PPO = polyphenol oxidase, NPO = NADP-dependent quinone oxidoreductase).
402 Percentage values in the QTL legends indicate the proportion of the observed variation
403 accounted for by the QTL.
404

Lines selected for consistently high or low levels of pinking and browning were grown in CE trials. Plants in CE had lower pinking and browning indices compared to those seen in field grown plants. Despite the fact that the lines responded consistently across field trials exposed to different environments, the reduced discolouration seen in CE suggests that environmental response may be a factor in the development of both pinking and browning. CE provided control of temperature, moisture availability, humidity and light availability. The spectrum of daylight, is likely to be different in wavelength profile and intensity to that produced in CE. Cultivar-level variation in abundance of some phenolic compounds in response to exposure to different wavelengths of light has previously been observed (Ouzounis *et al.,* 2015; Koukounaras *et al.,* 2016) and UV light exposure has been shown to influence discolouration specifically (reviewed in Hunter *et al.,* 2017). Consequently, a larger pool of phenolic compounds may have been available as substrates for discolouration reactions in field-grown material compared to CE-grown plants. Despite the overall reduction in discolouration in CE-grown material [3-fold browning index, 24-fold pinking index], the selected lines grouped into the same high and low pinking and browning categories as identified in the field trials.

3.3 Transcriptome analysis

Transcripts showing 3-fold or greater differential expression between samples expressing high and low levels of pinking or browning are indicated in Table S2, whilst those transcripts located between flanking markers for the identified QTL corresponding to pinking, browning or general discolouration are extracted in Table 3.

Table S2. Predicted proteins of transcripts up or down regulated in association with pinking or browning discolouration in mature field grown heads and 8 week post-planting material grown in controlled environment indicating fold increase (+) or decrease (-) in expression relative to non-discoloured material, predicted pathways and association with mapped discoloration QTL.

	Phenotype						
	Field		CE		Co-locating		
Predicted protein	**P**	**B**	**P**	**B**	**QTL**	**UniProt ID**	**Pathway or function**
2-hydroxyphytanoyl-CoA lyase			**+4**			Q54DA9	fatty acid metabolism
3-ketoacyl-CoA synthase			**+3**			Q9SIX1	fatty acid metabolism
3-ketoacyl-CoA synthase 6-like protein	**-3**				D1	A0A2J6LVF7	fatty acid metabolism
3-ketoacyl-CoA synthase 5-like protein		**+4**			B2	A0A2J6LY96	fatty acid metabolism
3-oxo-5-α-steroid 4-dehydrogenase	**-29**				B5	PLY89462	fatty acid metabolism
3-oxoacyl-[ACP] synthase	**-10**	**-6**			B2	A0A2J6JNU8	fatty acid metabolism
α-dioxygenase 1			**-3**		B1	Q9SGH6	fatty acid metabolism
β-ketoacyl synthase	**-8**					PLY86066	fatty acid metabolism
Acyl-ACP thioesterase		**+6**				PLY61749	fatty acid metabolism
Acyl-CoA desaturase	**-5**					A0A2J6MGF8	fatty acid metabolism
Acyl-CoA 5-desaturase AL21			**+3**		P2	P0DOW3	fatty acid metabolism
Acylhydrolase	**+11**	**+12**			D2	PLY91815	fatty acid metabolism
Acyltransferase	**+5**	**-11**			B2	A0A2J6KS02	fatty acid metabolism
Acyl transferase		**+4**			D2	A0A2J6K2S6	fatty acid metabolism
Class 3 Lipase		**-5**				PLY97470	fatty acid metabolism
COBRA-like lipoprotein synthetase		**+6**				A0A2J6LPG0	fatty acid metabolism

Enoyl-(ACP) reductase	**+7**	**-4**			B1	PLY97084	fatty acid metabolism
Enoyl-CoA reductase			**+5**			Q9M2U2	fatty acid metabolism
Epoxide hydrolase	**+4**					A0A2J6MEQ5	fatty acid metabolism
Ethanolamine-phosphate cytidylyltransferase	**+3**				P6	Q9ZVI9	fatty acid metabolism
Fatty acyl-CoA reductase		**+15**			B1	A0A2J6JP17	fatty acid metabolism
Fatty acid synthesis O_2 transporter			**-3**			O24521	fatty acid metabolism
Glutathione S-transferase		**+3**			B4	P32110	fatty acid metabolism
Glycerol phosphate acyltransferase			**+3**			Q9CAY3	fatty acid metabolism
Lecithin:cholesterol acyltransferase		**+4**			B1	A0A2J6MH62	fatty acid metabolism
Lipid transfer protein	**+12**	**+16**	**+5**		D2	PLY95206	fatty acid metabolism
Palmitoyl-monogalactosyldiacylglycerol δ-7 desaturase			**+3**	**+3**	P2	Q949X0	fatty acid metabolism
Phosphatidic acid phosphatase		**-3**				PLY62165	fatty acid metabolism
Omega-3 fatty acid desaturase			**+3**		B4	P48620	fatty acid metabolism
Tensin phosphatase		**-11**			D2	PLY74890	fatty acid metabolism
Very-long-chain enoyl-CoA reductase				**+4**	B2	Q9M2U2	fatty acid metabolism
Alkane hydroxylase MAH1-like			**-5**		B3	A0A2J6JZ74	wax biosynthesis
α-mannosidase		**+3**			B1	Q9LFR0	sugar metabolism
α-mannosyltransferase		**+17**			B5	A0A2J6LGJ2	sugar metabolism
β-galactosidase	**-3**				B4	Q9C6W4	sugar metabolism
Alginate lyase	**+8**	**+8**				PLY89994	sugar metabolism
Exostosin		**+11**			B2	PLY73645	sugar metabolism
Glucan endo-1,3-β-D-glucosidase	**-4**				B3	Q94G86	sugar metabolism
Glucose/ribitol dehydrogenase	**-6**	**-5**			P5	PLY77463	sugar metabolism

Glycoside hydrolase family 2, 9, 17, 47		**-5**				PLY84636	sugar metabolism
Glycosyl hydrolase family 1		**+19**			B5	PLY77220	sugar metabolism
Glycosyl hydrolase family 10	**+16**	**+8**				PLY76647	sugar metabolism
Glycosyl transferase family 8		**+3**			B1	A0A2J6JG41	sugar metabolism
Glycosyl transferase 61		**-4**				PLY67859	sugar metabolism
Invertase	**+16**					PLY86527	sugar metabolism
NAD dependent epimerase		**-11**			B1	A0A2J6KB13	sugar metabolism
Pectate lyase	**-5**		**-3**		D2	PLY64620	sugar metabolism
Phosphoenolpyruvate carboxylase kinase			**+3**			Q9SPK4	sugar metabolism
Phosphoglucose isomerase	**-4**					PLY72051	sugar metabolism
Sucrose synthase	**+5**		**+4**			P49039	sugar metabolism
UDP-glycosyltransferase 76C3		**+3**			B2	Q9FI96	sugar metabolism
Xylose isomerase	**-3**	**-3**			B4	Q9FKK7	sugar metabolism
Carbohydrate-binding protein (ER)	**+10**					PLY63356	sugar binding
EP1-like glycoprotein 4				**+3**	B3	A0A2J6M017	carbohydrate transport
Sucrose permease			**+4**			Q9FE59	sugar transport
Sugar transport protein		**+4**			B2	O04249	sugar transport
Sugar carrier protein C	**-3**				B2	Q41144	trans-membrane transport
Sugar transporter MSSP2			**+4**			Q8LPQ8	trans-membrane transport
α-expansin-8	**+3**				B2	O22874	structural
Acyl-Esterase	**-4**					A0A2J6M0M4	structural
ADF-cofilin-like protein		**+14**				PLY94096	structural
Cellulose synthase A			**+3**			A2Y0X2	structural

DnaJ 11 chaperone protein-like				**-3**	D1	A0A2J6M976	structural
Dynein light chain	**-3**				B5	PLY65182	structural
Expansin-A1	**-3**				B2	Q9C554	structural
Fasciclin-like arabinogalactan protein 12			**-5**	**-3**	B1	A0A2J6M5I9	structural
Formin-like protein			**+4**			Q84ZL0	structural
Glucomannan 4-β-mannosyltransferase 2	**+3**	**+3**			B1	Q9FNI7	structural
Kinesin	**-7**				D2	PLY73801	structural
KIP1-like protein	**-8**					A0A2J6M0M4	structural
Xyloglucan endotransglucosylase			**-4**	**-4**		P35694	structural
Pectin methylesterase 11	**+3**				B2	Q9SIJ9	structural
Pectin methylesterase inhibitor 61		**+3**			B2	Q9FK05	structural
Rho GTPase activation protein		**-5**				PLY90965	structural
Sulfated surface glycoprotein 185			**+3**			P21997	structural
Villin		**-7**				PLY96337	structural
Xyloglucan endotransglucosylase/hydrolase 22	**+3**				B4	Q38857	structural
Xyloglucan endotransglucosylase/hydrolase 25		**+4**			B4	Q38907	structural
7.3 kDa class II heat shock protein	**+3**				D2	O82013	protein metabolism
Aspartic acid proteinase inhibitor		**+283**			P5	A0A2J6JI63	protein metabolism
Aspartic peptidase		**-3**			D1	PLY86033	protein metabolism
Aspartic peptidase			**-4**		P6	A0A2J6LUS2	protein metabolism
Carboxypeptidase Y		**+4**	**+4**		B1	O13849	protein metabolism
Chloroplast 50S ribosomal protein 5			**+4**			P27684	protein metabolism
Cyclophilin-like peptidyl-prolyl isomerase	**-9**				D2	PLY63056	protein metabolism

Cysteine protease		**+56**			B1	A0A2J6JXM3	protein metabolism
E3 ubiquitin-protein ligase	**+4**				B4	Q6R567	protein metabolism
F-box protein, CPR1-like				**-4**	D1	A0A2J6K198	protein metabolism
GPI-anchor transamidase		**-6**				PLY82490	protein metabolism
Isoaspartyl peptidase/L-asparaginase				**-3**		Q8GXG1	protein metabolism
Metacaspase-1			**+3**			Q7XJE6	protein metabolism
Metalloendoproteinase		**-3**			D1	PLY77300	protein metabolism
Neprosin	**-281**					PLY64833	protein metabolism
Prolyl oligopeptidase	**+21**	**+10**			B2	A0A2J6L9H3	protein metabolism
Protein kinase	**-4**				B2	PLY85533	protein metabolism
Protein methyltransferase		**+3**			B2	PLY97876	protein metabolism
RING-type Zinc finger protein	**-3**				B4	PLY73739	protein metabolism
Serine carboxypeptidase		**+4**	**+4**		B4	PLY92695	protein metabolism
Sec1-like protein	**-5**				D2	PLY73377	protein transport
OPT oligopeptide transporter protein		**+9**			P3	PLY91943	protein transport
Dor1-like family		**+3**				PLY67518	protein trafficking
Calcineurin-like phosphoesterase		**+7**			B1	PLY77054	protein-membrane association
6-phosphogluconate dehydratase	**-488**	**-1877**				PLY86887	Ile & Val metabolism
Isovaleryl-CoA dehydrogenase	**-3**				B1	Q9SWG0	Ile & Val metabolism
Proline dehydrogenase	**-5**	**-8**				PLY62544	Pro & Arg metabolism
Carbamoyl-phosphate synthase	**-12**				B2	PLY87126	Arg metabolism
Amino-acid N-acetyltransferase		**+7**			B5	A0A2J6LRI9	Phe metabolism
3-deoxy-7-phosphoheptulonate synthase	**+3**					P29976	Phe, Tyr & Trp metabolism

Chorismate synthase	**+3**				B2	P27793	Phe, Tyr & Trp metabolism
Prephenate dehydratase	**+11**					PLY90159	Phe, Tyr & Trp metabolism
Tryptophan synthase		**-4**				PLY89119	Trp metabolism
Ribose-phosphate pyrophosphokinase		**-7**				PLY87838	Trp & His metabolism
Formiminotransferase		**+4**				PLY67712	His metabolism
Histidinol dehydrogenase	**-5**				B2	PLY90756	His metabolism
Cobalamin-independent methionine synthase	**+4**	**+7**			B1	Q42699	Met metabolism
Homocysteine methyltransferase			**+5**			Q42699	Met metabolism
Methylthioribose phosphate isomerase	**-42**					PLY86711	Met metabolism
Glutamine Dumper	**+6**	**+6**			D1	PLY84188	amino acid (Glu) export
14-3-3 protein	**-34**				P3	PLY80337	signaling
Arabinogalactan protein 10			**+4**			Q9M0S4	signaling
Auxin responsive protein-like	**-3**				B4	PLY91906	signaling
Auxin-induced protein 15A-like protein			**-4**	**-3**	B4	A0A2J6LX65	signaling
Auxin induced protein 15A-like protein	**+4**				B4	PLY91854	signaling
Auxin-responsive protein SAUR19-like				**-7**	B4	A0A2J6LWY8	signaling
Auxin-responsive protein SAUR21	**-3**				B4	Q9FJF9	signaling
Auxin-responsive protein SAUR21-like				**-4**	B4	A0A2J6LX59	signaling
Farnesyltransferase			**+3**			Q38920	signaling
Fasciclin-like arabinogalactan			**+4**			Q66GR0	signaling
Flotillin family protein		**-11**				A0A2J6JLU1	signaling
Hydroxyproline-rich arabinogalactan 31			**+4**			Q9FZA2	signaling
Inositol bisphosphate phosphatase			**+4**			Q42546	signaling
Phosphatidylethanolamine-binding protein		**-6**				PLY70464	signaling

Phosphatidylinositol kinase		**+5**			D2	PLY68809	signaling
Phosphatidylinositol-phospholipase C		**+3**			P3	A0A2J6M2A7	signaling
Phosphoinositide phosphatase		**-3**				PLY86410	signaling
Rapid Alkalinization Factor (RALF)	**+5**	**+4**			B5	PLY95818	signaling
ABC transporter G family				**+4**	P3	XP_023731515	trans-membrane transport
Adenine/guanine permease AZG1				**+3**	B2	A0A2J6KAH8	trans-membrane transport
Al activated malate transporter	**+4**					A0A2J6MED5	trans-membrane transport
Ammonium transporter			**+4**			O04161	trans-membrane transport
Auxin efflux carrier component 2	**+3**				B4	Q9LU77	trans-membrane transport
Auxin transporter	**+4**				B4	Q8L883	trans-membrane transport
Ctr copper transporter	**-4**					A0A2J6KK95	trans-membrane transport
Cyclic nucleotide-gated ion channel			**+3**			O65718	trans-membrane transport
DETOXIFICATION Protein 32			**+3**			F4I4Q3	trans-membrane transport
Potassium ion channel KAT3	**-84**	**+98**	**-4**		B1	PLY62631	trans-membrane transport
Sodium/calcium exchanger protein	**-17**					A0A2J6JR49	trans-membrane transport
Sulfate permease		**+4**				PLY61735	trans-membrane transport
Vacuolar iron transporter			**+3**			Q9M2C0	trans-membrane transport
WAT1-related protein At3g02690		**+3**			B4	Q93V85	trans-membrane transport
WAT1-related protein At5g40240	**-3**				B4	Q9FL08	trans-membrane transport
Xanthine/uracil/vitamin C permease	**-6**	**-6**			P4	PLY67115	trans-membrane transport
Zn transporter	**-7**	**-10**	**+5**			PLY66784	trans-membrane transport
β-1,3-glucanase			**+3**			Q9M069	stress response

Germin		**-7**			D2	A0A2J6LK00	stress response
Glutathione S-transferase	**+8**	**+15**			B2	PLY67369	stress response
Zinc finger stress-associated protein 8-like			**+4**		B2	A0A2J6LY68	stress response
Alcohol dehydrogenase			**-3**			Q8LEB2	stress response (cold, water)
Dehydration-responsive element-binding protein	**+6**	**+4**			B2	Q9FJ93	stress response (cold, water)
Dehydrin	**-5**			**+3**	D1	A0A2J6LA41	stress response (cold, water)
Late embryogenesis abundant protein	**-5**				P3	A0A2J6JP42	stress response (cold, water)
Raffinose synthase			**+4**			Q5VQG4	stress response (cold)
Choline phosphatase			**+3**			Q41142	stress response (salinity)
Mechanosensitive ion channel		**+4**			B4	PLY99544	stress response (mechanical)
D-mannose binding lectin		**+3**			D2	A0A2J6MF85	stress response (biotic)
Gamma-thionin protein family	**+36**					PLY80357	stress response (biotic)
Thaumatin	**-5**					A0A2J6KVT9	stress response (biotic)
Carbonic anhydrase	**-8**	**-15**	**-4**			F4JIK2	C capture
Ribulose bisphosphate carboxylase	**-10**	**-19**			B2	PLY77539	C capture
Chlorophyll a-b binding protein			**+5**			P27489	photosynthesis
Oxygen-evolving enhancer protein			**+4**			P85194	photosynthesis
Photosynthetic reaction protein		**-5**				PLY63935	photosynthesis
Photosystem II protein D1		**-3**			B4	A7Y395	photosynthesis
Chloroplastic magnesium-chelatase			**+5**			B8ANF1	chlorophyll synthesis
Porphobilinogen synthase			**+4**			Q9SFH9	chlorophyll synthesis
Chlorophyllase-2		**+3**			B4	Q9M7I7	chlorophyll degredation
Geranylgeranyl reductase	**+4**					Q9CA67	carotenoid biosynthesis
WEB family protein		**-3**			D1	PLY97322	chloroplast movement

Light-Regulated WD		**+3**		B1	Q9LPV9	photoperiod sensing
Cupredoxin			**+4**		P29602	electron transport
Cytochrome P450-like protein		**+24**		D2	PLY94036	electron transport
Cytochrome P450 CYP72A219			**-3**	B3	H2DH21	electron transport
Cytochrome P450 709B2			**-4**	B3	F4IK45	electron transport
Cytochrome P450 94A2			**+3**	B4	P98188	electron transport
Mavicyanin			**+5**		P80728	electron transport
NADH dehydrogenase			**+3**		Q8RWA7	electron transport
Photosynthetic NDH subunit 1			**+3**	B2	O80634	electron transport
Photosystem II D1 protein			**+3**	D1	PLY88491	electron transport
Pyridine cytochrome reductase	**+20**	**+4**			PLY91291	electron transport
Quinone oxidoreductase			**+3**	B4	P28304	electron transport
Uclacyanin-3			**+5**		Q96316	electron transport
Umecyanin			**+5**		P42849	electron transport
Cupredoxin			**+4**		P29602	electron transport
2-oxoacid dehydrogenases acyltransferase		**+7**			PLY65660	energy
Aconitase	**-246**			B2	PLY88014	energy
Alternative oxidase	**-17**			P3	A0A2J6LNS1	energy
Fe-dependent oxoglutarate dioxygenase	**-7**	**-11**		B1	Q9FXV6	energy
Isocitrate lyase	**-3**	**-3**		B4	P49297	energy
Malate synthase	**-5**				A0A2J6KHZ8	energy
Malic enzyme	**+1137**	**+1451**			PLY97373	energy
Phosphoglycerate kinase			**+4**		Q9LD57	energy

Pyruvate decarboxylase			**+4**			Q9FFT4	energy
2-oxoacid dependent dioxygenase			**+5**			Q9SKK4	oxidation
Aldo/keto reductase		**+5**			B1	A0A2J6MJ46	oxidation
Ascorbate peroxidase	**-8**					PLY69103	oxidation
Glucose-methanol-choline oxidoreductase		**+5**				PLY72830	oxidation
Glycine dehydrogenase			**+4**			Q94B78	oxidation
Nitrite/Sulfite reductase	**-6**					PLY84996	oxidation
Nucleotide-disulphide oxidoreductase	**-17**	**-10**			D2	PLY82910	oxidation
Catalase			**+5**			P45739	peroxidation
Auxin-responsive protein SAUR23-like			**+4**	**+7**	D1	A0A2J6KJR4	regulatory
Auxin-responsive protein SAUR50-like				**+6**	D1	A0A2J6L9H8	regulatory
BED-type Zinc finger protein			**-3**		D2	A0A2J6K2R0	regulatory
Diketo-phosphopentane phosphatase	**-4**	**-9**				A0A2J6LQC7	regulatory
GRF-type zinc finger protein	**+3**				B4	PLY79713	regulatory
Kinesin-like protein		**+3**			D1	PLY91413	regulatory
Nudix hydrolase 20	**-3**				B4	Q8VXZ0	regulatory
Nudix hydrolase 21	**+3**				B4	Q8VY81	regulatory
Trypsin inhibitor protease		**-8**				PLY85894	regulatory
Acidic endochitinase	**+3**				B2	P29024	plant defense
Adenosylhomocysteinase			**+6**			O23255	plant defense
Chitinase			**+3**			Q7Y1Z0	plant defense
Disease resistance protein At3g14460-like			**+61**		D1	A0A2J6LFH9	plant defense

Disease resistance protein – like protein	**+5**				D1	PLY80535	plant defense
LRR receptor-like serine/threonine-protein kinase FLS2			**-3**		B4	A0A2J6LFU1	plant defense
LRR receptor-like serine/threonine protease		**-5**			B4	PLY68176	plant defense
RP-13-like disease resistance protein	**+3**				B2	PLY97856	plant defense
Alcohol dehydrogenase-like		**+3**			B3	Q9FH04	developmental
Cytokinin dehydrogenase 3	**-3**				D2	Q9LTS3	developmental
Cytokinin hydroxylase	**+3**				B3	Q9FF18	developmental
Glutaredoxin-like protein At5g39865-like			**-3**		B4	A0A2J6KF66	developmental
Light-dependent short hypocotyls 4-like	**+3**	**+3**			D1	PLY96215	developmental
Pectin methylesterase			**+3**			O04886	developmental
Pectinesterase inhibitor	**-4**		**+3**			Q9FK05	developmental
Phosphoribosyltransferase		**-7**			B1	PLY87838	developmental
2-methyl-6-phytyl-1,4-hydroquinone methyltransferase	**+3**				B4	P23525	phenylpropanoid pathway
Caffeic acid 3-O-methyltransferase			**+3**			Q43239	phenylpropanoid pathway
Polyphenol oxidase	**+25**					P43309	phenylpropanoid pathway
Phenylalanine ammonia-lyase			**+3**			O04058	phenylpropanoid pathway
Shikimate kinase		**+3**			B1	PLY86265	phenylpropanoid pathway
Abscisic acid 8'-hydroxylase				**-4**		Q9LJK2	phenolic metabolism
Acetyl-CoA-benzylalcohol acetyltransferase			**-4**			O64988	phenolic metabolism
Alcohol acetyltransferase		**+3**				PLY83872	phenolic metabolism

Carotenoid oxygenase	**-5**					PLY66686	phenolic metabolism
Vanillyl-alcohol oxidase		**+9**				PLY67945	phenolic metabolism
Anthocyanidin 3-O-glucosyltransferase 2			**+3**		P3	A0A2J6LF68	flavonoid biosynthesis
Flavonol synthase		**+3**			B3	Q9M547	flavonoid biosynthesis
Kaempferol 3-O-β-D-galactosyltransferase	**+5**	**+3**			P5	Q9SBQ8	flavonoid biosynthesis
Malonyl-Co A: anthocyanin 3-O-glucoside-6'-O-malonyltransferase				**+3**	B3	A0A2J6JQ78	flavonoid biosynthesis
Naringenin-chalcone synthase	**+6**	**+7**		**-4**		P48387	flavonoid biosynthesis
(-)isopiperitenol/(-)carveol dehydrogenase				**+3**	B4	A0A2J6LKE0	terpenoid synthesis
3-hydroxy-3-methylglutaryl-CoA reductase	**+3**				B4	P14891	terpenoid synthesis
3-hydroxy-3-methylglutaryl-CoA reductase		**+3**			B4	P29057	terpenoid synthesis
Diphosphocytidyl-methyl-erythritol kinase			**+3**			P93841	terpenoid synthesis
Germacrene A synthase short form	**-3**				B4	Q8LSC2	terpenoid synthesis
Hydroxy-methylglutaryl-CoA reductase			**+3**			P48020	terpenoid synthesis
Terpene synthase	**+16**	**+30**			B3	PLY99643	terpenoid synthesis
Costunolide synthase			**+3**			F8S1I0	sesquiterpene lactone synthesis
Oxidosqualene cyclase		**+19**				A0A2J6KHJ6	sterol biosynthesis
Squalene monooxygenase			**+3**			O48651	sterol biosynthesis
Secologanin synthase	**+3**	**+3**			B3	Q05047	alkaloid synthesis
Strictosidine synthase		**-5**			P5	A0A2J6JPZ2	alkaloid synthesis

Caffeoylshikimate esterase			**+5**			Q9C942	lignin production
Laccase (diphenol oxidase) 6	**-7**	**-5**			B1	Q9ZPY2	lignin production
Peroxidase 47	**-3**				P6	Q9SZB9	lignin production
Aspartate racemase	**-4**					A0A2J6MED5	stereochemistry
Dirigent protein-like protein	**-4**	**-13**		**-8**	B2	Q9SS03	stereochemistry
Dirigent protein 4	**-3**		**-3**		D1	A0A2J6K9W1	stereochemistry
Dirigent protein 23	**+3**	**+3**			B4	Q84TH6	stereochemistry
Dirigent protein 23-like protein				**-6**	B4	A0A2J6KKV6	stereochemistry
Aquaporin	**-7**			**+8**	P3	Q41951	water transport
Aquaporin PIP1-1		**+3**			B2	P61837	water transport
Aquaporin PIP1-3	**-3**	**+3**			B2	Q08733	water transport
Aquaporin PIP1-6	**-3**				B2	Q9ATN0	water transport
Glutamate 5-kinase	**+7**				B2	PLY91259	nitrogen metabolism
Glutamine amidotransferase		**+3**			B2	A0A2J6LYQ3	nitrogen metabolism
High-affinity nitrate transporter	**-7**					A0A2J6LPZ0	nitrogen metabolism
Nodulin-like protein		**-6**			B1	PLY84544	nitrogen metabolism
BAHD acyltransferase	**-3**				B2	Q9FF86	general metabolism
Carboxylesterase			**+3**			Q9LT10	general metabolism
FMN-dependent α-hydroxy acid dehydrogenase	**-8**					PLY86997	general metabolism
Glyoxalase	**-9**				B1	A0A2J6LXD6	general metabolism

S-adenosyl-L-methionine-dependent methyltransferase	**+4**				D1	PLY80743	general metabolism
Cytolysin	**+6**					A0A2J6M2V0	cell death
Rhodanese like protein		**-8**				A0A2J6LBJ5	senescence
Senescence regulator S40	**-11**				B1	A0A2J6KPX2	senescence
Cellulase	**+3**					A0A2J6L3X4	membrane degradation
DREPP polypeptide		**-8**			B4	PLY83953	membrane synthesis
Mn/Fe superoxide dismutase	**-3**					PLY90327	antioxidant
Peroxiredoxin-2E-1			**+5**			Q69TY4	antioxidant
VIT family protein	**+4**	**+7**				PLY95029	iron transport
Ferritin-3	**+3**				B4	Q948P6	iron regulation
BES1/BZR1 Transcription factor	**+9**		**+4**		B5	PLY76419	transcription
bZIP transcription factor		**-3**			D1	PLY84189	transcription
E2FC Transcription factor	**-3**				P5	Q9FV70	transcription
EN 41Transcription factor	**+3**				B4	Q2HIV9	transcription
EN 42Transcription factor	**+4**				B4	Q700E3	transcription
ERF024 Ethylene-responsive transcription factor				**+3**	B2	A0A2J6LYE8	transcription
ERF098 Ethylene-responsive transcription factor			**-4**		P6	A0A2J6KGI9	transcription
Ethylene-responsive transcription factor		**-3**			B2	Q40476	transcription

Ethylene-responsive transcription factor		**-3**			B2	Q8L9K1	transcription
GATA transcription factor 1			**+3**			P69781	transcription
GRAS Transcription factor	**-20**	**-30**			B2	PLY90803	transcription
K-box Transcription factor		**-51**				PLY86436	transcription
MTERF6 Transcription terminator			**+3**			Q9SZL6	transcription
MYB1R1 Transcription factor			**+3**			Q2V9B0	transcription
MYB15Transcription factor	**-3**	**-4**			B4	Q9LTC4	transcription
Myc-type transcription factor		**+3**			B4	PLY77035	transcription
RLTR1Transcription factor		**+3**			B4	Q7XBH4	transcription
SBP-box type transcription factor	**+3**					A0A2J6K871	transcription
Scarecrow-like protein			**+3**			Q9FYR7	transcription
SRF-type transcription factor	**-4**	**+6**			B1	PLY79523	transcription
SWI3C Transcription regulator			**+3**			Q9XI07	transcription
TCP Transcription factor		**+52**			B1	PLY65615	transcription
TFIID Transcription initiation factor		**+49**			B1	PLY74721	transcription
WRKY transcription factor			**+3**		B2	Q93WU8	transcription
YABBY protein		**+6**			D2	PLY84293	transcription
Zinc-finger protein 6-like protein				**+3**	D1	A0A2J6K6I6	transcription
Zinc finger protein 6-like protein			**+4**		D1	A0A2J6LV52	transcription
Light-Dependent Short Hypocotyls 3-like				**+3**	B4	A0A2J6JQ41	transcription (light dependent)
Elongation factor 2		**+6**	**+7**		D2	Q9ASR1	translation
Elongation factor Ts			**-4**			A8G4D2	translation
Rho termination factor	**-5**					PLY75611	translation
RNA polymerase mediator subunit 4		**+4**			B4	PLY80754	translation
Translation elongation factor EF-1		**+5**			B1	PLY82430	translation

Translation initiation factor 4γ			**+3**		Q10475	translation
Malectin		**+5**			PLY72360	post-translational modification
Aminocyclopropane-carboxylate synthase	**-5**				A0A2J6JS65	ethylene synthesis
Formate--tetrahydrofolate ligase	**-3**			B1	P28723	C1 metabolism
Taurine catabolism dioxygenase	**+5**	**+6**			A0A2J6JTE9	sulfur metabolism
Purple acid phosphatase	**+4**				PLY84579	phosphorus metabolism
Inositol polyphosphate phosphatase	**+8**		**-4**		Q8H0Z6	light response
BYPASS1-related protein		**-4**		B4	PLY76197	plant architecture
Lysine-specific demethylase JMJ30			**+3**		Q8RWR1	flowering
Cupin	**+4**	**+8**		D2	A0A2J6KPM1	seed storage protein
Casparian strip membrane protein	**-5**				A0A2J6JLE0	extracellular diffusion
Exocyst component 84		**+5**		B3	A0A2J6KUY4	import
Cyclic nucleotide- and calmodulin-regulated ion channel 5		**+3**		B1	Q8RWS9	Calcium regulation
Stomagen	**-3**				A0A2J6LWN5	stomatal density
S-adenosylmethionine decarboxylase		**+3**			PLY77611	polyamine synthesis
Pinin-like protein		**+3**		B4	PLY94011	cell-cell adhesion
Thioredoxin H9	**+3**	**+3**		B4	Q9C9Y6	cell-cell communication
Topoisomerase		**+4**		B1	PLY97476	DNA replication
Maturase K		**-3**		B1	PLY86761	RNA processing
ADIPOR1 transmembrane protein			**+4**		B7F9G7	unknown
Major latex protein	**-9**				PLY84050	unknown

Matrixin	**-7**	PLY77300	unknown
TMPIT-like protein	**+4**	A0A2J6MJD7	unknown

+, upregulation in association with discolouration; - , down regulated in association with discolouration; P, pinking discolouration; B, browning discolouration; CE, controlled environment conditions.

437 **Table 3.** Selected transcripts grouped by the QTL under which they were located, showing increase (+) or decrease (-) in transcription relative to
438 non-discoloured material, association with pinking or browning discolouration in field and controlled environment produced plants, fold change
439 in transcript levels and predicted pathways.
440

		Phenotype					
		Field		CE			
QTL	**Predicted protein**	**P**	**B**	**P**	**B**	**UniProt ID**	**Pathway or function**
D1	Glutamine Dumper	**+6**	**+6**			PLY84188	amino acid (Glu) export
	Dehydrin	**-5**			**+3**	A0A2J6LA41	stress response (cold, water)
	Dirigent protein 4	**-3**		**-3**		A0A2J6K9W1	stereochemistry
	bZIP transcription factor		**-3**			PLY84189	transcription
D2	Cytochrome P450-like protein		**+24**			PLY94036	electron transport
	Nucleotide-disulphide oxidoreductase	**-17**	**-10**			PLY82910	oxidation
	Elongation factor 2		**+6**	**+7**		Q9ASR1	translation
	Germin		**-7**			A0A2J6LK00	stress response
	YABBY protein		**+6**			PLY84293	transcription
	Pectate lyase	**-5**		**-3**		PLY64620	sugar metabolism
B1	Potassium ion channel KAT3	**-84**	**+98**	**-4**		PLY62631	trans-membrane transport
	TCP Transcription factor		**+52**			PLY65615	transcription
	TFIID Transcription initiation factor		**+49**			PLY74721	transcription
	NAD dependent epimerase		**-11**			A0A2J6KB13	sugar metabolism

	Laccase (diphenol oxidase) 6	**-7**	**-5**			Q9ZPY2	lignin production
	Cobalamin-independent methionine synthase	**+4**	**+7**			Q42699	Met metabolism
	SRF-type transcription factor	**-4**	**+6**			PLY79523	Transcription
	Aldo/keto reductase		**+5**			A0A2J6MJ46	oxidation
	Translation elongation factor EF-1		**+5**			PLY82430	translation
	α-dioxygenase 1			**-3**		Q9SGH6	fatty acid metabolism
	α-mannosidase		**+3**			Q9LFR0	sugar metabolism
	Glycosyl transferase family 8		**+3**			A0A2J6JG41	sugar metabolism
	Isovaleryl-CoA dehydrogenase	**-3**				Q9SWG0	Ile & Val metabolism
	Shikimate kinase		**+3**			PLY86265	phenylpropanoid pathway
B2	GRAS Transcription factor	**-20**	**-30**			PLY90803	transcription
	Glutathione S-transferase	**+8**	**+15**			PLY67369	stress response
	Dirigent protein-like protein	**-4**	**-13**		**-8**	Q9SS03	stereochemistry
	Carbamoyl-phosphate synthase	**-12**				PLY87126	Arg metabolism
	Exostosin		**+11**			PLY73645	sugar metabolism
	Dehydration-responsive element-binding protein	**+6**	**+4**			Q9FJ93	stress response (cold, water)
	Histidinol dehydrogenase	**-5**				PLY90756	His metabolism
	Sugar transport protein		**+4**			O04249	sugar transport
	UDP-glycosyltransferase 76C3		**+3**			Q9FI96	sugar metabolism
	Sugar carrier protein C	**-3**				Q41144	trans-membrane transport
	Chorismate synthase	**+3**				P27793	Phe, Tyr & Trp metabolism
	ERF024 Ethylene-responsive transcription factor				**+3**	A0A2J6LYE8	transcription

	Ethylene-responsive transcription factor		**-3**			Q40476	transcription
	Ethylene-responsive transcription factor		**-3**			Q8L9K1	transcription
	WRKY transcription factor			**+3**		Q93WU8	transcription
	Adenine/guanine permease AZG1				**+3**	A0A2J6KAH8	trans-membrane transport
	Aquaporin PIP1-1		**+3**			P61837	water transport
	Aquaporin PIP1-3	**-3**	**+3**			Q08733	water transport
	Aquaporin PIP1-6	**-3**				Q9ATN0	water transport
B3	Terpene synthase	**+16**	**+30**			PLY99643	terpenoid synthesis
	Glucan endo-1,3-β-D-glucosidase	**-4**				Q94G86	sugar metabolism
	Secologanin synthase	**+3**	**+3**			Q05047	alkaloid synthesis
	EP1-like glycoprotein 4				**+3**	A0A2J6M017	carbohydrate transport
	Flavonol synthase		**+3**			Q9M547	flavonoid biosynthesis
	Malonyl-Co A: anthocyanin 3-O-glucoside-6'-O-malonyltransferase				**+3**	A0A2J6JQ78	flavonoid biosynthesis
B4	Dirigent protein 23-like protein				**-6**	A0A2J6KKV6	stereochemistry
	MYB15Transcription factor	**-3**	**-4**			Q9LTC4	transcription
	EN 42Transcription factor	**+4**				Q700E3	transcription
	Mechanosensitive ion channel		**+4**			PLY99544	stress response (mechanical)
	Dirigent protein 23	**+3**	**+3**			Q84TH6	stereochemistry
	Xylose isomerase	**-3**	**-3**			Q9FKK7	sugar metabolism
	(-)isopiperitenol/(-)carveol dehydrogenase				**+3**	A0A2J6LKE0	terpenoid synthesis
	2-methyl-6-phytyl-1,4-hydroquinone methyltransferase	**+3**				P23525	phenylpropanoid pathway

	3-hydroxy-3-methylglutaryl-CoA reductase	**+3**				P14891	terpenoid synthesis
	3-hydroxy-3-methylglutaryl-CoA reductase		**+3**			P29057	terpenoid synthesis
	β-galactosidase	**-3**				Q9C6W4	sugar metabolism
	EN 41Transcription factor	**+3**				Q2HIV9	transcription
	Germacrene A synthase short form	**-3**				Q8LSC2	terpenoid synthesis
	Glutathione S-transferase		**+3**			P32110	fatty acid metabolism
	Myc-type transcription factor		**+3**			PLY77035	transcription
	NADH-quinone oxidoreductase		**-3**			PLY87786	phenylpropanoid pathway
	RLTR1Transcription factor		**+3**			Q7XBH4	transcription
B5	3-oxo-5-α-steroid 4-dehydrogenase	**-29**				PLY89462	fatty acid metabolism
	Glycosyl hydrolase family 1		**+19**			PLY77220	sugar metabolism
	α-mannosyltransferase		**+17**			A0A2J6LGJ2	sugar metabolism
	BES1/BZR1 Transcription factor	**+9**		**+4**		PLY76419	transcription
	Amino-acid N-acetyltransferase		**+7**			A0A2J6LRI9	Phe metabolism
P3	Aquaporin	**-7**			**+8**	Q41951	water transport
	Late embryogenesis abundant protein	**-5**				A0A2J6JP42	stress response (cold, water)
	Anthocyanidin 3-O-glucosyltransferase 2			**+3**		A0A2J6LF68	flavonoid biosynthesis
P4	Xanthine/uracil/vitamin C permease	**-6**	**-6**			PLY67115	trans-membrane transport
P5	Glucose/ribitol dehydrogenase	**-6**	**-5**			PLY77463	sugar metabolism
	Kaempferol 3-O-β-D-galactosyltransferase	**+5**	**+3**			Q9SBQ8	flavonoid biosynthesis

	Strictosidine synthase		**-5**	A0A2J6JPZ2	alkaloid synthesis
	E2FC Transcription factor	**-3**		Q9FV70	transcription
P6	ERF098 Ethylene-responsive transcription factor		**-4**	A0A2J6KGI9	transcription
	Peroxidase 47	**-3**		Q9SZB9	lignin production

441 +, upregulation in association with discolouration; - , down regulated in association with discolouration; D, overall discolouration P, pinking

442 discolouration; B, browning discolouration; CE, controlled environment condition

443 Differential transcript analyses between lines showing either pinking or browning
444 discolouration and the respective non-discolouring lines at harvest (day 0) were made
445 from RNA samples from the extreme lines grown under CE conditions (Table 2) and
446 subsequently from the identified consistent lines from July- and September- harvested
447 trials from 2016.

448 Although the majority of differentially expressed transcripts were not shared
449 between the two discolouration types, some commonality was indicated, suggesting the
450 involvement of the same metabolic pathways in both cases (Figure 4).

451 Figure 4

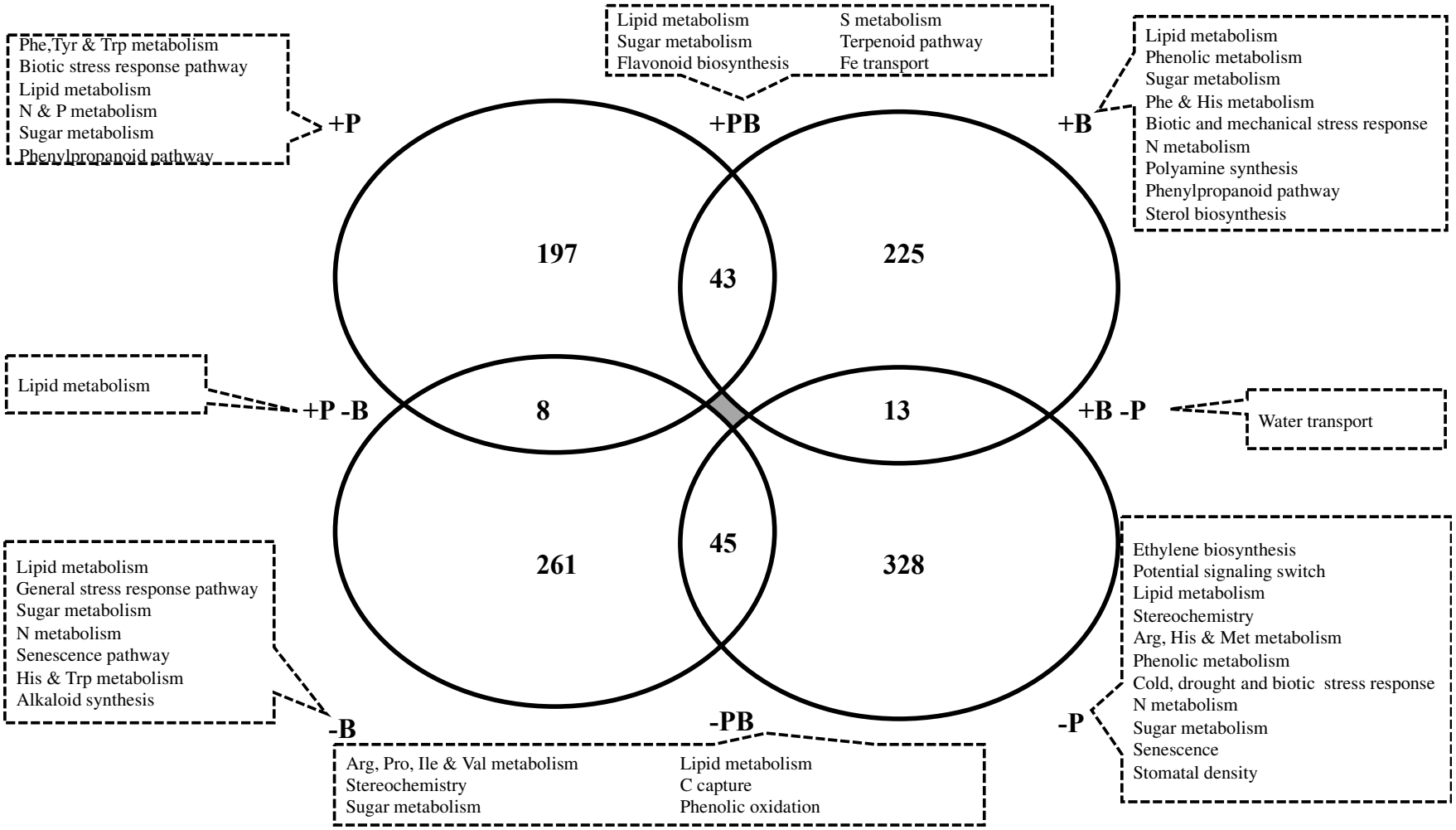

452

Figure 4. Diagrammatic representation of the total numbers of transcripts associated with each different phenotype expression pattern. +P indicates transcripts expressed more highly in pinking, +B indicates transcripts expressed more highly in browning, -P and -B indicate transcripts expressed more strongly in material showing low levels of discolouration (pinking and browning respectively). Categories with only one letter (i.e. P+, rather than P+ B+) indicate transcripts differentially expressed in association with one type of discolouration but not differentially expressed in association with the other, whilst those categories with two letters indicate differential expression associated with both types of discolouration. Call-out boxes indicate typical processes and pathways associated with each category.

3.4 Transcripts located under discolouration QTL

Based on data from the CE trials, primers were designed for qRT-PCR for abscisic acid hydrolase 4, chalcone synthase, PAL and PPO, trans-cinnamate 4-monooxygenase, chalcone-flavonone isomerase, flavonoid-3'-monooxygenase and NAD(P)H-quinone oxidoreductase. qRT-PCR was performed on RNA from field trials 5 and 7 and used to map QTL for all transcripts showing significant variation. QTL for PAL and PPO and NAD(P)H-quinone oxidoreductase co-located with QTL for browning on LG 8a (PAL) and LG 9b (PPO and NAD(P)H-quinone oxidoreductase (Figure 3).

Additional investigation of transcript localization under each of the QTL for discolouration identified a low temperature and drought stress response protein, late embryogenesis abundant protein-like, transcripts associated with the flavonoid and alkaloid pathways, anthocyanidin 3-O-glucosyltransferase (EC 2.4.1.115); kaempferol 3-O-β-D-galactosyltransferase (EC 2.4.1.234) and strictosidine synthase, peroxidase and aquaporin underlying QTL for pinking. A number of transcripts involved in the phenylpropanoid, flavonoid, terpene and alkaloid synthesis, Phe metabolism: chorismate synthase; amino acid N-acetyl transferase, polysaccharide synthesis: glycosyl transferase family 8 and exostosin, a mechanosensitive ion channel, stereochemistry associated functions: dirigent-like proteins and an NAD-dependent epimerase [EC 5.1.3.2], and additional aquaporin genes were found underlying QTL for browning.

Transcripts involved in stress response (e.g. dehydrin) and stereochemistry (dirigent-like proteins) were also located under QTL associated with general discolouration. It is notable that the genomic regions underlying QTL associated with pinking contained a number of genes for which a reduction in transcript expression was associated with browning and *vice versa* (Table 3).

Transcripts for strictosidine synthase showed reduced expression associated with increased browning but was located underneath a QTL for pinking, whilst the gene for Carbamoyl-phosphate synthase (EC 6.3.4.16), showing reduced transcription in association with pinking was located underneath a QTL for browning. This suggests that the pathways resulting in pinking or browning may, in-part, be interrelated, potentially with the same or similar substrates being utilized in different ways.

In addition to enzyme transcripts, a number of transcription factors were identified as being differentially expressed and several of these were detected underlying QTL for pinking and browning. Specifically, BEZ/BRZ type transcription factors were highly expressed in association with pinking, whilst SRF-type transcription factors showed reduced expression in association with pinking and increased expression in association with browning. These two types of transcription factor were found underlying browning QTL 1 and 5, as was a TCP type transcription factor highly expressed in association with browning. Transcription factor types TFIID and YABBY were also found to be highly expressed in association with browning and were found underlying browning QTL 1 and discolouration QTL 2. This would indicate that the transcription level regulation may be important in control of the processes which lead to the development of discolouration, particularly browning.

3.4.1 Transcripts associated with pinking

Transcripts for polyphenol oxidase (PPO) (EC 3.10.3.1) and several enzymes in the phenylpropanoid pathway including phenylalanine ammonia lyase (PAL) (EC 3.4.1.24), the key enzyme responsible for regulating the initial stages of the pathway in plants showed increased expression in plants which subsequently developed high pinking indices compared to those that did not. This was to be expected as PAL activity

515 has been shown to be induced in response to wounding in plant tissues (Hyodo *et al.,*
516 1978; López-Galvez *et al.,* 1996; Peiser *et al.,* 1998; Hisaminato *et al.,* 2001), but these
517 transcripts did not show increased expression associated with the development of
518 browning. In addition to PAL and PPO, other transcripts strongly associated with
519 pinking included anthocyanidin 3-O-glucosyltransferase 2, involved in anthocyanin
520 biosynthesis; 3-hydroxy-3-methylglutaryl-CoA reductase (EC 1.1.1.88) and 4-
521 diphosphocytidyl-2-C-methyl-D-erythritol kinase (EC 2.7.1.148) involved in caffeoyl
522 Co-A, isoprenoid biosynthesis; and caffeic acid 3-O-methyltransferase (EC 2.1.1.68)
523 and caffeoylshikimate esterase (EC 3.1.1.-), involved in biosynthesis of caffeic acid
524 derivatives, suggesting the involvement of the phenylpropanoid pathway, specifically
525 caffeic acid.

526 In addition, transcripts of acetyl-CoA-benzylalcohol acetyltransferase (EC
527 2.3.1.224) were found to show reduced expression in association with pinking. This
528 enzyme directs carbon away from the phenylpropanoid pathway by converting
529 phenylpyruvate into benzyl acetate instead of phenylalanine. In field-grown material,
530 increased expression of transcripts corresponding to 3-deoxy-7-phosphoheptulonate
531 synthase (EC 2.5.1.54) and prephenate dehydratase (EC 4.2.1.51), which are associated
532 with the assimilation of chorismate into the phenylpropanoid pathway, were also
533 associated with pinking.

534 Pinking was also associated with increased expression of transcripts for
535 costunolide synthase EC 1.14.14.150), squalene monooxygenase (EC 1.14.14.17),
536 farnesyltransferase (EC 2.5.1.58) and 2-methyl-6-phytyl-1,4-hydroquinone
537 methyltransferase (EC 2.1.1.295), all of which are involved in terpenoid,
538 sequiterpenoid and plant steroid production, and with reduced expression of
539 germacrene A synthase (EC 4.2.3.23) and carotenoid oxygenase (EC 1.13.11.69).

These latter two enzymes are involved in production of sesquiterpenes compounds involved in the development of bitterness and plant defence (Chadwick *et al*., 2013, Chadwick *et al*., 2016) and break-down of carotenoid products of the terpene synthesis pathway respectively. Reduced expression of these transcripts may represent reduced pull-through of resources to these particular endpoints of the terpenoid pathway. Moreover, squalene monooxygenase diverts terpenoid backbone components away from sesquiterpenoid and toward triterpenoid and steroid biosynthetic pathways.

In field-produced material, transcripts encoding sucrose synthase (EC 2.4.1.13), invertase (EC 3.2.1.26) and phosphoenolpyruvate carboxylase kinase (EC 4.1.1.32), involved in the interconversion of sucrose, glucose and fructose showed increased expression in association with pinking, whilst those encoding phosphoglucose isomerase (EC 5.3.1.9), β-galactosidase (EC 3.2.1.23) and glucan endo-1,3-β-D-glucosidase (EC 3.2.1.39), which act on more complex sugars, showed reduced expression. The simple sugars are precursors of the glycolysis cycle which feeds into terpenoid biosynthesis and into the production of non-polar aliphatic amino acids, whilst metabolism of complex sugars would tend to divert resources away from these pathways and is associated with the production of charged aliphatic amino acids in particular arginine. Transcription of enzymes associated with biosynthesis of aromatic amino acids, derived from the shikimate pathway, also showed increased expression in association with pinking.

Saltveit (2018), suggested that the level of pinking observed is dependent on the relative proportion of caffeic acid accumulated in the cells before the action of PPO commences after processing, with higher levels of caffeic acid resulting in more production of caffeoyl-*o*-quinone, which is pink, as opposed to other *o*-diphenols which produce greenish quinones. The overall colour can also be influenced by the amino

565 acids with which *o*-quinones subsequently react and by the levels of antioxidants (AO)
566 which re-convert the *o*-quinones back to their respective *o*-diphenols. The pathways
567 highlighted by the data produced in this study agrees with the Saltveit (2018) model, in
568 that increased transcription of enzymes which promote production of *p*-coumaryl-CoA
569 within the phenylpropanoid pathway should drive the pathway toward production of
570 caffeic acid and thus induce pinking. However, the data we have produced suggests the
571 involvement of at least two other pathways: 1) the flavonoid biosynthesis pathway,
572 which diverts *p*-coumaroyl-CoA away from the production of caffeic acid toward the
573 production of naringenin-chalcone, and 2) the terpenoid biosynthetic pathway, which
574 diverts chorismite, a precursor molecule of the phenylpropanoid pathway, into tyrosine
575 production. According to the model, both of these pathways should reduce pinking as
576 they direct the phenylpropanoid pathway away from caffeic acid production. Our data
577 however shows aspects of both of these pathways associated with the development of
578 both browning and pinking. It is possible that components of these other pathways
579 perform the cycling function of antioxidants (AO) in the Saltveit (2018) model.
580 Damerun *et al.* (2015) have shown that flavanone 3-hydroxylase, involved in the
581 biosynthesis of the flavonoids, is strongly associated with AO activity and that such
582 activity correlated with shelf-life of plant material. However, this was not the case for
583 the carotenoids which were negatively correlated with AO activity. The precise nature
584 of the interaction of these compounds and their impact on discolouration still remains
585 unclear.

586 The other component of the Saltveit model is the amino acids with which the *o*-
587 quinones react. Our data suggests that up-regulation of transcripts in pathways that
588 would likely lead to increased levels of proline, may be associated with the
589 development of pinking. Proline has been associated with expression of stress related

590 genes (Hare *et al.,* 1999, Wang *et al.,* 2015) and in protection against oxidative damage
591 Djabou *et al.* (2017). Accumulation of proline in response to oxidative damage in
592 lettuce may increase availability of proline for interaction with *o*-quinones in the
593 development of pinking. The amino acid tyrosine (Tyr) is synthesized from chorismate
594 and feeds into the biosynthesis of the terpenoid backbone. The direction of chorismate
595 toward the phenylpropanoid pathway would also tend to direct material away from
596 synthesis of Tyr and the terpenoid backbone.

597 As well as diphenols, PPO is able to convert Tyr into dopaquinone. The
598 interaction of quinones with compounds including amino acids is thought to be the
599 source of the discolouration pigmentation in both pinking and browning (Hunter *et al.,*
600 2017; Saltveit, 2018). Hence, enzyme activities which alter the balance of amino acids
601 available for interaction are also likely to influence the final discolouration. In addition
602 to Tyr, genes for enzymes involved in biosynthesis of tryptophan (Trp) i.e. 3-deoxy-7-
603 phosphoheptulonate synthase, chorismate synthase and prephenate dehydratase,
604 showed increased expression in association with pinking, whilst other genes in this
605 pathway (tryptophan synthase and ribose-phosphate pyrophosphokinase [EC 2.7.6.1])
606 showed reduced expression in association with browning.

607 Genes involved in the metabolism of histidine (histidinol dehydrogenase
608 [EC1.1.1.23]) and arginine (carbamoyl-phosphate synthase) were identified as showing
609 reduced expression in association with pinking. The expression of genes for other
610 enzymes involved in the biosynthesis of histidine (ribose-phosphate
611 pyrophosphokinase [reduced expression] and formiminotransferase (EC 2.1.5.2)
612 [increased expression]) were also associated with browning. Both pinking and
613 browning were associated with reduced expression of transcripts for proline
614 dehydrogenase (EC 1.5.5.2); this enzyme converts proline into pyrroline carboxylate,

615 consequently reduced expression of this enzyme would tend to increase available
616 proline for interaction with quinones.
617
618 3.4.2 Transcripts associated with browning
619 Expression of transcripts for shikimate kinase (EC2.7.1.71), which promotes
620 conversion of Trp to chorismite, which subsequently feeds into the phenylpropanoid
621 pathway, was increased in association with browning as were transcripts for amino-acid
622 N-acetyltransferase (EC 2.3.1.36), involved in Phe metabolism. Conversely, transcripts
623 for tryptophan synthase (EC 4.2.1.20) and strictosidine synthase, both of which are
624 involved in the production of alkaloids, a process which directs chorismate away from
625 the phenylpropanoid pathway, showed reduced expression in association with
626 browning.
627 Transcripts representing flavonol synthase (EC 1.14.11.23) and malonyl-Co A:
628 anthocyanin 3-O-glucoside-6'-O-malonyltransferase (EC 2.3.1.171), key components
629 of the flavonoid biosynthesis pathway and specifically anthocyanin production, also
630 showed increased expression in association with browning. Transcripts associated with
631 genes in the carotenoid pathway i.e. abscisic acid 8'-hydroxylase (EC1.14.13.93),
632 associated with the production of phaseic acid, showed reduced expression. This would
633 suggest that the phenylpropanoid pathway is involved with browning as well as pinking
634 although there is an indication that push-through of resources to the flavonoid pathway
635 is favoured in the development of browning.
636 An increase in the biosynthesis of dicaffeoyltartaric, 3,5-dicaffeoylquinic and
637 particularly chlorogenic (5-caffeoylquinic) acids in lettuce has been linked to tissue
638 wounding (Tomás-Barberán *et al.,* 1997; Cantos *et al.,* 2002) and more recently
639 increased levels of 5-*trans*- and 5-*cis*-chlorogenic acids at harvest have been associated

640 with subsequently increased browning in processed Romaine lettuce (García *et al.,*
641 2018, García *et al.,* 2019). The up-regulation of the transcription of genes for shikimate
642 hydroxycinnamoyl transferase (EC 2.3.1.133) (involved in the assimilation and
643 subsequent conversion of *p*-coumaroyl-CoA to caffeoyl-CoA via caffeoylquinic acid)
644 in association with pinking discolouration under CE conditions in this study agrees with
645 these findings. In contrast to García et al., (2018 & 2019), we identified an increase in
646 transcription of caffeic acid *o*-methyltransferase (EC 2.1.1.68), involved in
647 sinapaldehyde synthesis, associated with development of pinking. Garcia *et al*., (2018
648 & 2019) focussed specifically on mid-rib tissue and analysed the biochemistry 5 days
649 post-processing, whilst our study used whole leaf material and investigated pre-existing
650 differences in transcript levels at harvest, subsequently associated with symptom
651 development. Transcript levels, and subsequent expression levels and concomitant
652 biochemistry, may have altered during storage. Moreover, the Garcia studies did not
653 differentiate between pink and brown discolouration, identifying all discolouration as
654 browning (Tomaś-Barberań, 2019, pers. comm.) and was based on Romaine lettuce
655 cultivars (and cultivar-specific differences between metabolite profiles) whilst our
656 work involved a RIL population from a cross between and iceberg and a batavian line.
657 Given the observed negative correlation between pinking and browning and the fact
658 that pinking was not measured by García *et al.* (2018 & 2019) this suggests that
659 increased expression of caffeic acid 3-O-methyltransferase may be associated with
660 reduced browning.

661 Despite the fact that other enzymes directly involved with metabolism of the
662 compounds identified by García *et al.* (2018 & 2019) were not found to be differentially
663 expressed in our work, many of the metabolic pathways indicated are similar;
664 specifically, the phenylpropanoid pathway, which is central to many secondary

665 metabolic processes in plant cells, the anthocyanin, terpenoid and isoprenoid pathways.
666 We associated up-regulation of transcripts in all of these pathways with increased
667 pinking, and by inference decreased browning, whilst García *et al.* (2019) suggested
668 that these latter three pathways would be responsible for directing carbon flow away
669 from chlorogenic acid production, resulting in decreased browning.

670 Transcripts associated with the terpenoid pathway that showed increased
671 expression in browning material included 3-hydroxy-3-methylglutaryl-CoA reductase
672 (EC 1.1.1.88), the rate-limiting enzyme in the cytoplasmic melavonate pathway, one of
673 two alternate pathways which leads to terpenoid biosynthesis. The other being the
674 chloroplastic MEP pathway (Lichtenthaler, 1999), (-)isopiperitenol/(-)carveol
675 dehydrogenase (EC 1.1.1.243) and oxidosqualene cyclase (EC 5.4.99.7) which are
676 involved specifically in monoterpene and triterpenoid biosynthesis respectively.

677 Transcripts for genes involved in complex sugar metabolism, in particular α-
678 mannosidase (EC 3.2.1.24) and α-mannosyltransferase (EC 2.4.x.x) and in
679 polysaccharide production: exostosin, glycosyl transferase families 8 and 61 (EC
680 2.4.2.x), were increased in association with browning. In addition, an NAD-dependent
681 epimerase, potentially involved with stereochemical interconversion of sugars showed
682 reduced expression. This suggests a role for stereochemical control of the sugar
683 metabolism pathways, particularly complex sugars, in the development of browning.
684 As noted previously, complex sugar metabolism is associated with the production of
685 charged aliphatic amino acids in particular arginine.

686 In addition to epimerase, other transcripts associated with regulation of
687 stereochemistry, specifically transcripts for a number of dirigent protein-like proteins
688 were also found to show differential expression in association with browning.

Browning was also associated with increased expression of transcripts encoding aquaporin and a potassium- ion channel protein (both which showed reduced expression in association with pinking). These may both be involved in water stress regulation and indicate an environmental influence on the development of browning. Furthermore, browning was associated with increased expression of transcripts for a mechanosensitive ion channel protein which may respond to physical damage.

3.5 Communally expressed transcripts

In field-grown material, increased levels of transcripts associated with metabolism of phenylalanine (Phe), one of the precursors to the phenylpropanoid pathway were associated with both pinking and browning discolouration. Laccase (EC 1.10.3.2) and peroxidase, which are involved in lignin production showed reduced transcription in lines exhibiting pinking or browning compared to respective non-discolouring lines. This would suggest that lignin production is not the endpoint of the pathway(s) leading to these discolourations and that the pathways resulting in either pinking or browning diverge at some point within the phenylpropanoid pathway.

Transcripts encoding naringenin-chalcone synthase (EC 2.3.1.74), an enzyme acting early in the flavonoid pathway converting *p*-coumaroyl-CoA to naringenin-chalcone and terpene synthase (EC 4.2.3.48), which acts in the sesquiterpenoid pathway were also highly transcribed in association with both pinking and browning in the field samples but not in the CE samples, with terpene synthase showing reduced expression in association with browning under CE conditions. Both of these enzymes have been associated with salt and osmotic stress tolerance (Wang *et al.,* 2018, Zhou *et al.,* 2020) in okra and rice respectively, indicating environmental influences on the expression of these genes.

In addition to the three major pathways identified, other functions associated with discolouration include increased expression of genes for the glutamine dumper protein. This protein has been shown to be involved in exudation of glutamine (Glu) from plant hydathodes (Pilot *et al.,* 2004), presumably resulting in a relative increase in the concentrations of other amino acid groups e.g. aromatic amino acids, as well as a non-selective reduction of amino acid concentration in cells and concomitant increase in concentration in the apoplast (Pratelli *et al*., 2020), where they would be available for rapid interaction with quinones released upon processing of the tissue. The release of material from hydathodes is likely to be influenced by water status of the plant, consequently the increased transcription of ion channel proteins, dehydrin and aquaporins observed in browning (and the reduced transcription observed in pinking) may also be associated with this process. Whether greater expression of water transport pore proteins results in increased water uptake or facilitates water loss, however, remains undetermined, however the observation by Monaghan *et al* (2016), that reduced water availability close to harvest has been shown to reduce rib-pinking suggests that reduced transcription of these transcripts may be associated with an overall increase in water status.

A number of other transcripts associated with response to drought stress and low temperature also showed variable expression in pinking, although different transcripts were identified in the CE and field samples. Higher expression of a subset of these genes were associated with pinking in the CE; reduced expression of a different subset was associated with pinking in field samples. This suggests that pinking may be more environmentally susceptible than browning.

Transcripts involved in the stereochemical control of reactions may also have a role to play: Aspartate racemase (EC 5.1.1.13) is responsible for the conversion of L-

739 Asp to D-Asp. L-Asp is involved in the production of coenzyme A (CoA), a key
740 component of the phenylpropanoid pathway. Reduced expression of aspartate racemase
741 (as identified in association with pinking), would suggest that more Asp would be in
742 the L-form and therefore available for conversion into CoA. Dirigent is thought to drive
743 the production of the lignin component (+)-pinoresinol, from the oxidation of two
744 coniferyl alcohol molecules (Davin *et al.,* 1997*).* Whilst the activity of dirigent itself is
745 limited to coniferyl alcohol oxidation (Kim *et al.,* 2002), and lignin production was not
746 associated with discolouration development in this study, other similar proteins could
747 potentially influence the stereochemistry of other oxidative reactions in the
748 phenylpropanoid or related pathways. Given the detection of differential transcription
749 in at least five proteins involved in stereoselection, it is possible that this is a mechanism
750 by which pathways leading to pinking and browning discolouration are differentiated.
751 Most of the pinking-associated transcripts identified as having a role in the
752 phenylpropanoid pathway are downsteam of the pathway converting coumaric acid to
753 coumaroyl alcohol. The pathways feeding into or out of this part of the
754 phenylpropanoid pathway would seem to be likely targets for any site of steroselective
755 activity. Coumaric acid exists in o-, m- and p- isomers, with p-coumaric acid
756 specifically involved in the phenylpropanoid pathway, however o-, and m-coumaric
757 acid have been shown to rapidly inhibit mushroom PPO (Kermasha *et al.,* 1993).
758 Inhibition of PPO is likely to result in reduced pinking and/or increased browning,
759 based on our observation of increased levels of PPO transcription associated
760 specifically with pinking. Furthermore, the immediate precursor of coumaric acid,
761 cinnamic acid exists as both cis- and trans- isomers. The enzyme which catalyses this
762 step, trans-cinnamate-4-monooxygenase (EC 1.14.1491), is trans-isomer specific. Cis-
763 cinnamic acid levels have been shown to be increased by exposure to light, particularly

764 UV in Arabidopsis (Wong *et al*., 2005). Increased UV would be associated with
765 increased sunlight and therefore temperature, which could result in increased water
766 stress. This in turn could lead to reduced pinking and/or increased browning, according
767 to the data presented in this study.
768
769 **4 Summary**

770 This work provides novel insight into the biochemical pathways and compounds which
771 influence post-harvest discolouration in lettuce and their underlying genetic control.
772 Using a population of F_7 RILs (Saladin x Iceberg) with previously reported variation in
773 the development of pinking and browning discolouration, we have observed that
774 pinking and browning phenotype are generally distinct traits under both genetic and
775 environmental control. The pinking and browning phenotypes observed 3 days post-
776 harvest were mapped on a revised Saladin x Iceberg genetic map to 6 QTL associated
777 with pinking, 5 QTL associated with browning and 2 QTL associated with general
778 discolouration.

779 Involvement of the phenylpropanoid pathway was indicated in the development
780 of both forms of discolouration, with conversion of coumaric acid to coumaryl alcohol
781 appearing to be the boundary step beyond which pinking developed. The association of
782 several transcripts involved in stereoselective processes suggest that stereochemical
783 selection, as a result of differential transcriptional control, may be involved in
784 regulating discolouration. The flavonoid and terpenoid biosynthesis pathways and other
785 peripheral biochemistry including amino acid metabolism were also found to be
786 involved (Figure 5). The fact that a number of differences in expression were only
787 observed in the field-grown samples suggest that environmental factors may play a role

788 in regulation of the transcription of some of these genes, and consequently in the
789 development of discolouration.

790 Figure 5

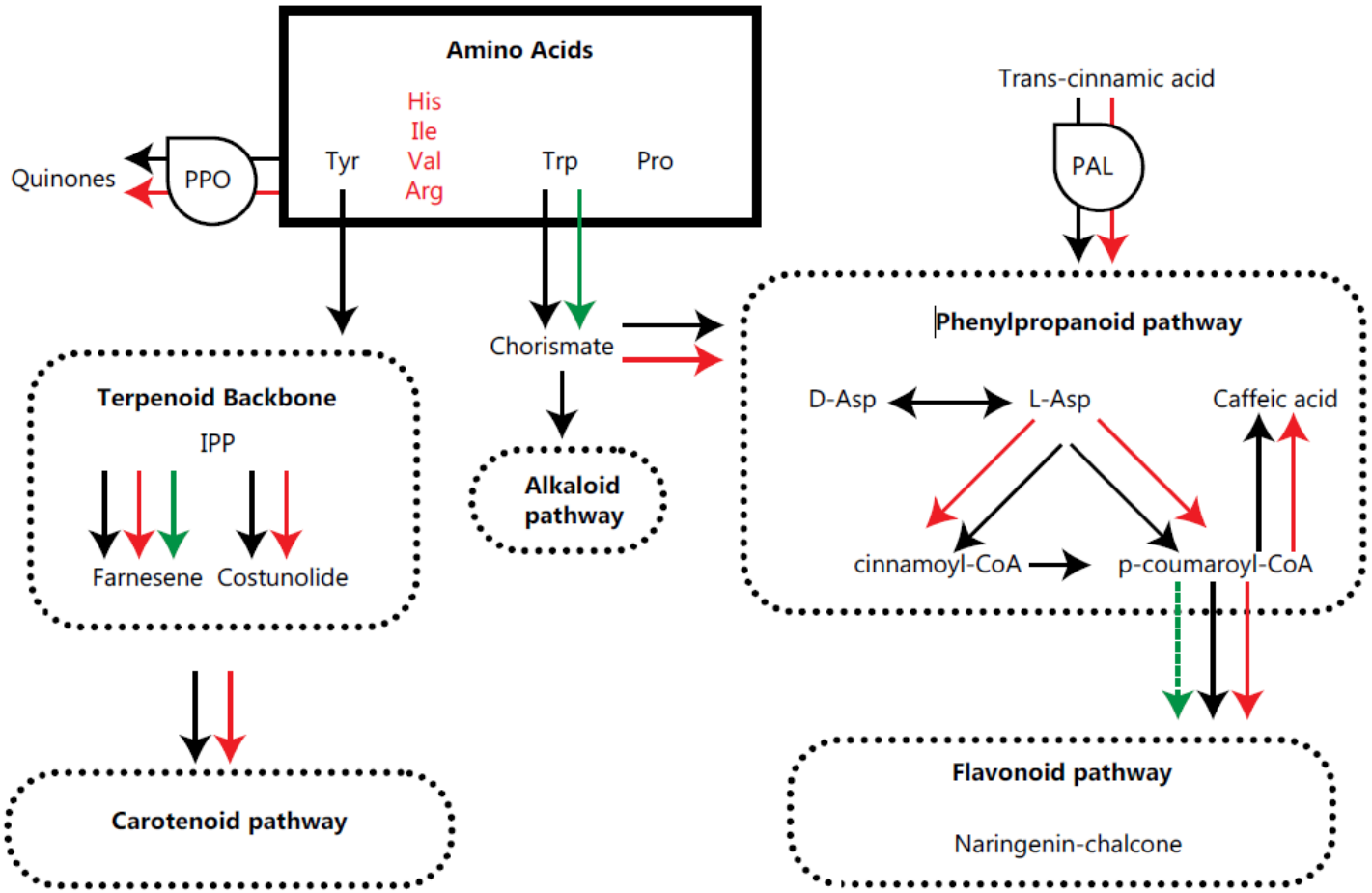

791

Figure 5. Simplified view of the pathways indicated as being involved in pinking and browning development in lettuce based on transcriptome profiles from field-grown and CE-grown material. Simplified pathways are shown in black. Red arrows indicate processes associated with pinking, green arrows indicate processes associated with browning.

5 Acknowledgements

We would like to thank Richard Stark for his invaluable statistical help and Rijk Zwaan, Gs growers, Bakkavor, AHDB, and HIP for their support. This work was funded under BBSRC HAPI (Grant No. BB/M017745/1)

6 References

ADAS. Irrigation Best Practice: A Water Management Toolkit for Field Crop Growers. 2007. Available from http://79.170.40.182/iukdirectory.com/iuk/pdfs/A Water Management Toolkit for Field Crop Growers.pdf. (Accessed 1/6/2015).

Altschul SF, Gish W, Miller W, Myers EW, Lipman DJ. 1990. Basic local alignment search tool. Journal of Molecular Biology **215**, 403-410.

Andrews S. (2010) FastQC: A quality control tool for high throughput sequence data. Available from http://www.bioinformatics.babraham.ac.uk/projects/fastqc/ (Accessed 28/5/2018)

Atkinson L, Hilton HW, Pink DAC. 2013a. A study of variation in the tendency for postharvest discolouration in a lettuce (*Lactuca sativa*) diversity set. International Journal of Food Science and Technology **48,** 801–807.

Atkinson LD, McHale LK, Truco MJ, Hilton HW, Lynn J, Schut JW, Mitchelmore RW, Hand P, Pink DAC. 2013b. An intra-specific linkage map of

lettuce (*Lactuca sativa*) and genetic analysis of postharvest discolouration traits. Theoretical and Applied Genetics **126,** 2737–2752.

Buchfink B, Xie C, Huson DH. 2015. Fast and sensitive protein alignment using DIAMOND. Nature Methods **12**, 59-60.

Bushnell B. BBMap. www.sourceforge.net/projects/bbmap/

Cantos JA, Tudela MI, Espín JC. 2002. Phenolic compounds and related enzymes are not rate-limiting in browning development of fresh-cut potatoes. Journal of Agriculture and Food Chemistry **50,** 3015–3023.

Damerun A, Selmes SL, Biggi GF et al. 2015. Elucidating the genetic basis of antioxidant status in lettuce (*Lactuca sativa*). Horticulture Research 2, 15055.

Davin LB, Wang HB, Crowell AL, *et al.* 1997. Stereoselective bimolecular phenoxy radical coupling by an auxiliary (dirigent) protein without an active center. Science. **275**, 362–366.

Defra. 2010. The Fertiliser Manual (RB209) 8th edition. The Stationery Office, London.

Degl'Innocenti E, Guidi L, Paradossi A, Tognoni F. 2005. Biochemical study of leaf browning in minimally processed leaves of lettuce (*Lactuca sativa* L. var. Acephala). Journal of Agriculture and Food Chemistry **53**, 9980–9984.

Djabou ASM, Carvalho LJCB, Li QX, Niemenak N, Chen S. 2017. Cassava postharvest physiological deterioration: a complex phenomenon involving calcium signaling, reactive oxygen species and programmed cell death. Acta Physiologiae Plantarum 3**9,** 91

Dobin A, Davis CA, Schlesinger F, Drenkow J, Zaleski C, Jha S, Batut P, Chaisson M, Gingeras TR. 2013. STAR: ultrafast universal RNA-seq aligner. Bioinformatics **29**, 15–21.

Ewels P, Magnusson M, Lundin S, Käller M. 2016. MultiQC: summarize analysis results for multiple tools and samples in a single report. Bioinformatics **32**, 3047–3048.

García CJ, Gil MI, Tomas-Barberan FA. 2018**.** LC–MS untargeted metabolomics reveals early biomarkers to predict browning of fresh-cut lettuce. Postharvest Biology and Technology. **146**, 9-17.

García CJ, Gil MI, Tomás-Barberán FA. 2019 Targeted metabolomics analysis and identification of biomarkers for predicting browning of fresh-cut lettuce. Journal of agricultural and food chemistry. **67(20)**, 5908-17.

Gawlik-Diziki U, Złotek U, Świeca M. 2008. Characterization of polyphenol oxidase from butter lettuce (*Lactuca sativa* var. capitata L.). Food Chemistry **107**, 129–135.

Hare PD, Cress WA, Staden J. 1999. Proline synthesis and degradation: a model system for elucidating stress-related signal transduction. Journal of Experimental Botany **50,** 413-434.

Hayes RJ, Galeano CH, Luo Y, Antonise R, Simko I. 2014. Inheritance of decay of fresh-cut lettuce in a recombinant inbred line population from 'Salinas 88' x 'La Brillante' Journal of the American Society for Horticultural Research **139**, 388–398.

Hilton HW, Clifford SC, Wurr DCE, Burton KS. 2009. The influence of agronomic factors on the visual quality of field-grown, minimally-processed lettuce. Journal of Horticultural Science and Biotechnology **84,** 193–198.

Hisaminato H, Murata M, Homma S. 2001. Relationship between enzymatic browning and phenylalanine ammonia lyase activity of cut lettuce, and the prevention of browning by inhibitors of polyphenol biosynthesis. Bioscience, Biotechnology and Biochemistry **65,** 1016–1021.

Huerta-Cepas J, Forslund K, Coelho LP Szklarczyk D, Jensen LJ, von Merring C, Bork P. 2017. Fast genome-wide functional annotation through orthology assignment by eggNOG-mapper. Molecular Biology and Evolution **34**, 2115–2122.

Hunter PJ, Atkinson LD, Vickers L, Lignou S, Oruna-Concha MJ, Pink D, Hand P, Barker G, Wagstaff C, Monaghan JM. 2017. Oxidative discolouration in whole-head and cut lettuce: Biochemical and environmental influences on a complex phenotype and potential breeding strategies to improve shelf-life. Euphytica **213**, 180.

Hyodo H, Kuroda H, Yang SF. 1978. Induction of phenylalanine ammonia-lyase and increase in phenolics in lettuce leaves in relation to their development of russet spotting caused by ethylene. Plant Physiology **62**, 31–35.

Jones P, Binns D, Chang HY *et al.* 2014. InterProScan 5: genome-scale protein function classification. Bioinformatics **30** 1236–1240.

Kays SJ. 1999. Preharvest factors affecting appearance. Postharvest Biology and Technology 1**5,** 233–247.

Kermasha S, Goetghebeur M, Monfette A. 1993. Studies on inhibition of mushroom polyphenol oxidase using chlorogenic acid as substrate. Journal of Agricultural and Food Chemistry **41,** 526-531

Kim MK, Jeon J-H, Fujita M, Davin LB, Lewis NG. 2002. The western red cedar (Thuja plicata) 8-8′ DIRIGENT family displays diverse expression patterns and conserved monolignol coupling specificity. Plant Molecular Biology. **49**, 199–214.

Koukounaras A, Siomos AS, Gerasopoulos D, Karamanoli K. 2016. Genotype, ultraviolet irradiation, and harvesting time interaction effects on secondary metabolites of whole lettuce and browning of fresh-cut product. Journal of Horticultural Science and Biotechnology **91,** 491–496.

Langmead B, Trapnell C, Pop M, Salzberg SL. 2009. Ultrafast and memory-efficient alignment of short DNA sequences to the human genome. Genome Biology. **10**, 10: R25.

Lee SK, Kader AA. 2000. Preharvest and postharvest factors influencing vitamin C content of horticultural crops. Postharvest Biology and Technology **20,** 207–220.

Li H, Handsaker B, Wysoker A, Fennell T, Ruan J, Homer N, Marth G, *Abecasis G*, *Durbin R*, 1000 Genome Project Data Processing Subgroup. 2009. *The Sequence Alignment/Map format and SAMtools*. Bioinformatics. **25**, 2078–2079.

Liao Y, Smyth GK, Shi W. 2014. FeatureCounts: an efficient general purpose program for assigning sequence reads to genomic features. Bioinformatics **30,** 923–930.

Lichtenthaler HK. 1999. The 1-Deoxy-D-xylulose-5-phosphate pathway of isoprenoid biosynthesis in plants. Annual Review of Plant Physiology and Plant Molecular Biology **50,** 47-65.

López-Galvez G, Saltveit M, Cantwell M. 1996. Wound-induced phenylalanine ammonia-lyase activity: factors affecting its induction and correlation with the quality of minimally processed lettuces. Postharvest Biology and Technology **9,** 223–233.

Love MI, Huber W, Anders S. 2014. Moderated estimation of fold change and dispersion for RNA-seq data with DESeq2. Genome Biology and Evolution **15,** 550.

Lyons E, Freeling M. 2008. How to usefully compare homologous plant genes and chromosomes as DNA sequences. The Plant Journal **53**, 661–673.

Madeira F, Park YM, Lee J *et al.* 2019. The EMBL-EBI search and sequence analysis tools APIs in 2019. Nucleic Acids Research, April 12, 2019; doi: 10.1093/nar/gkz268

Martin M. 2011. Cutadapt removes adapter sequences from high-throughput sequencing reads. EMBnet.journal. **17**, 10–12.

Martinez MV, Whitaker JR. 1995. The biochemistry and control of enzymatic browning. Trends in Food Science and Technology **6,** 195–200.

Monaghan JM, Vickers LH, Grove IG, Beacham AM. 2016. Deficit irrigation reduces postharvest rib pinking in wholehead Iceberg lettuce, but at the expense of head fresh weight. Journal of the Science of Food and Agriculture 97, 1524-1528.

Ouzounis T, Parjikolaei BR, Fretté X, Rosenqvist E, Ottosen C-O. 2015. Pre-dawn and high intensity application of supplemental blue light decreases the quantum yield of PSII and enhances the amount of phenolic acids, flavonoids, and pigments in *Lactuca sativa* Frontiers in Plant Science **6,** 19.

Peiser G, López-Gálvez G, Cantwell M, Saltveit ME. 1998. Phenylalanine ammonia lyase inhibitors control browning of cut lettuce. Postharvest Biology and Technology **14,** 171–177.

968 **Pilot G, Stransky H, Bushey DF, Pratelli R, Ludewig U, Wingate VP, Frommer**
969 **WB** (2004) Overexpression of GLUTAMINE DUMPER1 leads to hypersecretion of
970 glutamine from hydathodes of *Arabidopsis* leaves. Plant Cell **16,** 1827–1840
971
972 **Pratelli R, Voll LM, Horst RJ, Frommer WB, Pilot G.** 2010. Stimulation of
973 nonselective amino acid export by glutamine dumper proteins. Plant Physiology **152**,
974 762-773.

975 **Pruitt KD, Tatusova T, Maglott DR.** 2005. NCBI Reference Sequence (RefSeq): a
976 curated non-redundant sequence database of genomes, transcripts and proteins. Nucleic
977 Acids Research **33**, D501–D504.
978
979 **Queiroz C, Lopes MLM, Fialho E, Valente-Mesquita L.** 2008. Polyphenol oxidase:
980 characteristics and mechanisms of browning control. Food Reviews International **24,**
981 361–375.
982
983 **Quinlan AR, Hall IM.** 2010. BEDTools: a flexible suite of utilities for comparing
984 genomic features. Bioinformatics. **26**, 841–842.
985
986 **R Core Team.** 2018. R: A language and environment for statistical computing. R
987 Foundation for Statistical Computing, Vienna, Austira. https://www.R-project.org/
988
989 **Saltveit M.** 2018. Pinking of lettuce. Postharvest Biology and Technology **145**, 41–
990 52.
991

992 **Sgamma T, Pape J, Massiah A, Jackson S.** 2016. Selection of reference genes for
993 diurnal and developmental time-course real-time PCR expression analyses in lettuce,
994 Plant Methods **12,** 21.

995 **Simko I, Hayes RJ, Truco M-J, Michelmore RW, Antonise R, Massoudi M.** 2018.
996 Molecular markers reliably predict post-harvest deterioration of fresh-cut lettuce in
997 modified atmosphere packaging. Horticulture Research **5**, 21.
998

999 **Soininen K.** 2009. Salads and salad dressings, UK. Mintel Group Ltd. London, UK.
1000

1001 **Solomon EI, Sundaram UM, Machonkin TE.** 1996. Multicopper oxidases and
1002 oxygenases. Chemistry Reviews **96,** 2563–2605.
1003

1004 **Tomás-Barberán FA, Loaiza-Velarde J, Bonfanti A, Saltveit ME**. 1997. Early
1005 wound- and ethylene-induced changes in phenylpropanoid metabolism in harvested
1006 lettuce. Journal of the American Society for Horticultural Science **122**, 399–404.
1007

1008 **Toivonen PMA, Brummell DA.** 2008. Biochemical bases of appearance and texture
1009 changes in fresh-cut fruit and vegetables. Postharvest Biology and Technology **48,** 1–
1010 14.
1011

1012 **Van Ooijen JW.** 2009. MapQTL 6, Software for the mapping of quantitative trait loci
1013 in experimental populations of diploid species. Kyazma B.V. Wageningen,
1014 Netherlands.
1015

Van Ooijen JW. 2018. JoinMap 5, Software for the calculation of genetic linkage maps in experimental populations of diploid species. Kyazma B.V., Wageningen, Netherlands.

Wang F, Ren G, Li F, Qi S, Xu Y, Wang B, Yang Y, Ye Y, Zhou Q, Chen X. 2018. A chalcone synthase gene *AeCHS* from *Abelmoschus esculentus* regulates flavonoid accumulation and abiotic stress tolerance in transgenic *Arabidopsis*. Acta Physiologiae Plantarum **40,** Article 97.

Wang H, Tang X, Wang H, Shao H-B. 2015. Proline accumulation and metabolism-related genes expression profiles in *Kosteletzkya virginica* seedlings under salt stress. Frontiers in Plant Science **29**. doi: org/10.3389/fpls.2015.00792

Wong WS, Guo D, Wang XL, Yin XQ, Xia B, Li N. 2005. Study of *cis*-cinnamic acid in *Arabidopsis thaliana*. Plant Physiology and Biochemistry **43,** 929-937.

Young MD, Wakefield MJ, Smyth GK, Oshlack A. 2010. Gene ontology analysis for RNA-seq: accounting for selection bias. Genome Biology **11,** R14.

Zawistowski J, Biliaderis CG, Eskin NAM. 1991. Polyphenoloxidase. In: Robinson DS, Eskin NAM, eds. Oxidative enzymes in foods. London: Elsevier Science, 217–273.

1041 **Zhou H-C, Shamala LF, Yi X-K, Yan Z, Wei S.** 2020. Analysis of Terpene
1042 Synthase Family Genes in *Camellia sinensis* with an Emphasis on Abiotic Stress
1043 Conditions. Scientific Reports **10,** Article 933.

Declaration of interests

☒ The authors declare that they have no known competing financial interests or personal relationships that could have appeared to influence the work reported in this paper.

☐The authors declare the following financial interests/personal relationships which may be considered as potential competing interests: